NASS
NAN YANG ACADEMY OF SCIENCES

Earth and Planetary Science
https://journals.nasspublishing.com/index.php/eps

ARTICLE

Fault Seal Integrity Assessment of the Bornu Basin Using Advanced Software Techniques

Chekwube Nnamdi Didi

Petroleum Geoscience Program, Pan African University Institute of Life and Earth Sciences (Including Health and Agriculture), University of Ibadan, Ibadan 200005, Nigeria

ABSTRACT

The Bornu Basin, located in northeastern Nigeria, is a sub-basin of the larger Chad Basin and has long been considered a prospective area for hydrocarbon exploration. Despite the presence of quality source rocks, favorable reservoir properties, and structural traps, exploration efforts have largely resulted in dry wells. This study investigates the fault seal integrity of the Bornu Basin as a potential explanation for this paradox. Using 3D seismic data and well logs from the Bulte-1 well, fault seal analysis was conducted with Move and Petrel software (2018 versions). Key techniques included the interpretation of fault geometries, stratigraphic modeling, and quantitative analyses such as Shale Gouge Ratio (SGR), Shale Smear Factor (SSF), Probabilistic SSF, Clay Smear Potential (CSP), and Hydrocarbon Column Height (HCCH) estimations. The F13 fault was identified as a regional structure of interest, and detailed analyses revealed heterogeneous sealing behavior along its plane. Results show that while some intervals demonstrate high sealing potential (high SGR and low permeability), other segments, particularly at greater depths, exhibit high fault throw, low smear continuity, and high leakage risk. These findings suggest that fault-related leakage and early hydrocarbon migration, possibly induced by tectonic or magmatic activity, are key factors limiting successful hydrocarbon entrapment in the basin. The study concludes that fault seal integrity is a

*CORRESPONDING AUTHOR:
Chekwube Nnamdi Didi, Petroleum Geoscience Program, Pan African University Institute of Life and Earth Sciences (Including Health and Agriculture), University of Ibadan, Ibadan 200005, Nigeria; Email: didichekwube@gmail.com

ARTICLE INFO
Received: 10 August 2025 | Revised: 17 September 2025 | Accepted: 20 September 2025 | Published Online: 2 October 2025
DOI: https://doi.org/10.36956/eps.v4i2.2752

CITATION
Didi, C.N., 2025. Fault Seal Integrity Assessment of the Bornu Basin Using Advanced Software Techniques. Earth and Planetary Science. 4(2): 56–80. DOI: https://doi.org/10.36956/eps.v4i2.2752

critical risk factor in the Bornu Basin, and integrating advanced fault modeling into exploration workflows is essential for future prospect evaluation.

Keywords: Bornu Basin; Fault Seal Integrity; Hydrocarbon Exploration; Shale Gouge Ratio (SGR); Move Software; Structural Trap Leakage

1. Introduction

The Nigeria Chad Basin (**Figure 1**), located in Borno State, Northeastern Nigeria, spans roughly 23,000 km^2 between latitudes 9°30′ N–13°40′ N and longitudes 11°45′ E–14°45′ E. It is separated from the Upper Benue Basin by the Zambuk Ridge [1]. Most of the Chad Basin lies beyond Nigeria, covering about 2.5 million km^2 across Chad, Libya, Niger, Sudan, Cameroon, and northern Nigeria. To date, around 23 exploratory wells and several 2D seismic surveys have been conducted in the Nigerian sector (**Figure 1**). Many wells drilled in the Bornu Basin have turned out dry, raising questions about why this is the case, especially given that geochemical studies confirm the presence of quality source rocks [2–4], reservoir assessments indicate favorable petrophysical properties [5,6], and structural mapping reveals numerous faulted structures and anticlines that could serve as effective traps [7]. Furthermore, adjacent basins in Niger and Chad have shown significant oil discoveries under similar conditions [8]. This suggests a need to investigate fault seal integrity to determine whether these traps are leaking. If the traps are intact, is it possible that hydrocarbons never migrated into them? Alternatively, could hydrocarbons have migrated but escaped before trap formation? If early leakage occurred, what geological event might have triggered it? Is there field evidence, such as oil stains, to support this scenario? Additionally, do the analogue basins share comparable sedimentary sequences and thicknesses with the Bornu Basin? If not, what are the implications for the petroleum system in the Bornu Basin? Several key geological and geodynamic factors can help explain this paradox.

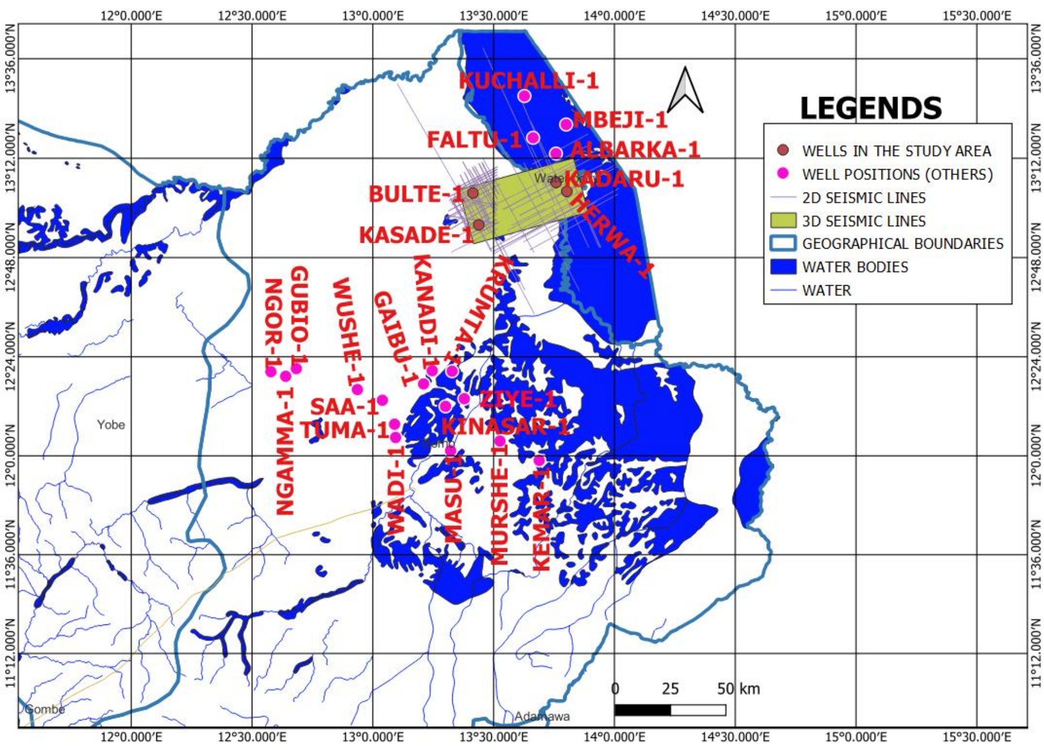

Figure 1. Map of Bornu Basin with 23 exploratory wells, seismic survey area, and drainage systems.

Source: Modified after Adekoya et al. [9].

Geochemical analyses confirm that formations like the Gongila and Fika Shales contain sufficient organic matter for hydrocarbon generation, with TOC values often exceeding the 0.5 wt% threshold and vitrinite reflectance values indicating maturity [9–11]. Fault planes in Bornu Basin are often steeply dipping and extensional in nature [12]. This can lead to open fractures that allow hydrocarbons to leak, making fault-related traps risky [7]. Fault seal analysis, such as stochastic juxtaposition modeling, is essential to accurately predict sealing capacity [13].

There is evidence that hydrocarbon generation in the Bornu Basin may have occurred before trap formation, possibly due to magmatic intrusions during the Late Cretaceous. These events caused early maturation and hydrocarbon migration, followed by loss through open faults before effective traps formed [14]. Oil seepages have been reported in the oldest stratigraphic units of Bornu Basin, like the Bima Sandstone, suggesting that hydrocarbons did migrate and possibly leaked to the surface [14].

Neighboring basins like Termit (Niger) and Doba (Chad) have greater sediment thickness (up to 15,000 m) and more consistent trap-seal relationships. These differences enhance hydrocarbon retention and commercial discoveries [15,16]. Intrusive magmatic activity and uplift events caused cooling and erosion, disrupting the normal maturation and entrapment processes [11,17]. Despite favorable source, reservoir, and trap conditions, Bornu Basin's dry wells are likely due to fault leakage, premature migration before trap formation, and magmatic or tectonic disturbances. Detailed fault seal analysis and deeper drilling strategies, as seen in neighboring basins, are essential next steps. Therefore, this study concentrates on analyzing fault seal integrity in the Bornu Basin by applying advanced tools available such as Petrel and Move Software (2018 version).

2. Geological Settings

The Bornu Basin, located in northeastern Nigeria, is a significant sub-basin (**Figure 2**) within the larger Chad Basin and forms part of the West and Central African Rift System (WCARS) [7,16,18–21]. Its geological setting reflects a complex history of tectonic, sedimentary, and structural processes tied to the breakup of Gondwana and the subsequent evolution of inland rift basins [16,22]. The Bornu Basin is a product of failed rifting and is classified as an aulacogen formed during the Mesozoic era from extensional tectonics when South America and Africa separated [7,23,24]. It is bounded by major faults trending predominantly NE-SW, ENE-WSW, and NW-SE, which were likely reactivated during tectonic episodes, such as the Santonian inversion [25–27]. The Bornu Basin features a well-defined stratigraphic succession (**Figure 3**) reflecting diverse depositional environments over time [28]. At the base lies the Bima Sandstone (Lower Cretaceous), composed of fluvial continental sandstones [29–31]. Above it, the Gongila Formation represents a marine to paralic environment with alternating shales and limestones. This is followed by the Fika Shale, a deeper marine unit rich in organic matter, indicating significant hydrocarbon potential. Overlying this is the Kerri-Kerri Formation (Tertiary), made up of continental sediments, and at the top is the Chad Formation (Quaternary), consisting of lacustrine (lake-derived) deposits [17,18]. The basin is characterized by horst and graben structures resulting from extensional faulting. Subsurface data reveal sedimentary thicknesses reaching up to 11.5 km in places, with several deep-seated faults acting as potential hydrocarbon migration pathways [32]. Depositional environments vary from high-energy fluvial systems to shallow marine and deltaic settings [23,33]. The sedimentary deposits in the basin show heterogeneity in lithology, including coarse-grained sandstones and finer shales, supporting hydrocarbon system development [34]. The basin has the fundamental elements for hydrocarbon accumulation: source rocks (organic-rich shales), reservoirs (sandstones), and seals (shales and carbonates). Organic matter is predominantly Type III kerogen, indicating a gas-prone system with localized oil potential [10,35]. Remote sensing, aeromagnetic, and seismic methods have enhanced the understanding of the basin's hidden structures. Depth to magnetic basement varies widely, and volcanic intrusions are common in the southern part of the basin [36]. The Bornu Basin is a complex rift-related geological system with a diverse stratigraphic and structural framework that supports hydrocarbon exploration[23,37–40]. Despite challenging surface conditions and mixed exploration results, its geological setting remains promising for further studies and potential resource development.

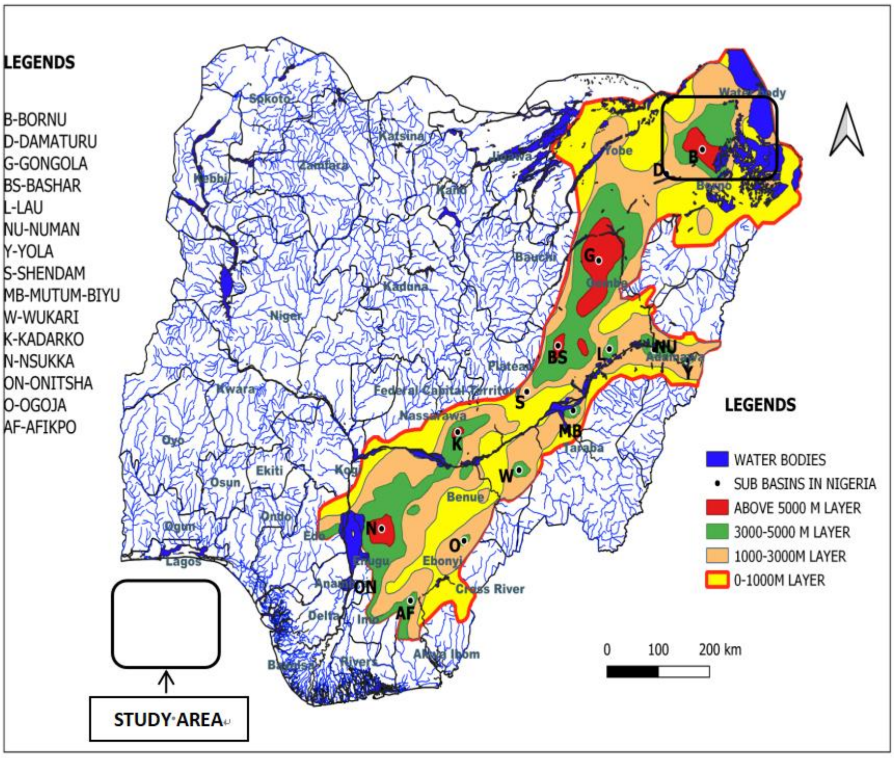

Figure 2. Map showing sub-sedimentary basins in Nigeria, including Bornu Basin. Source: Didi et al.[12].

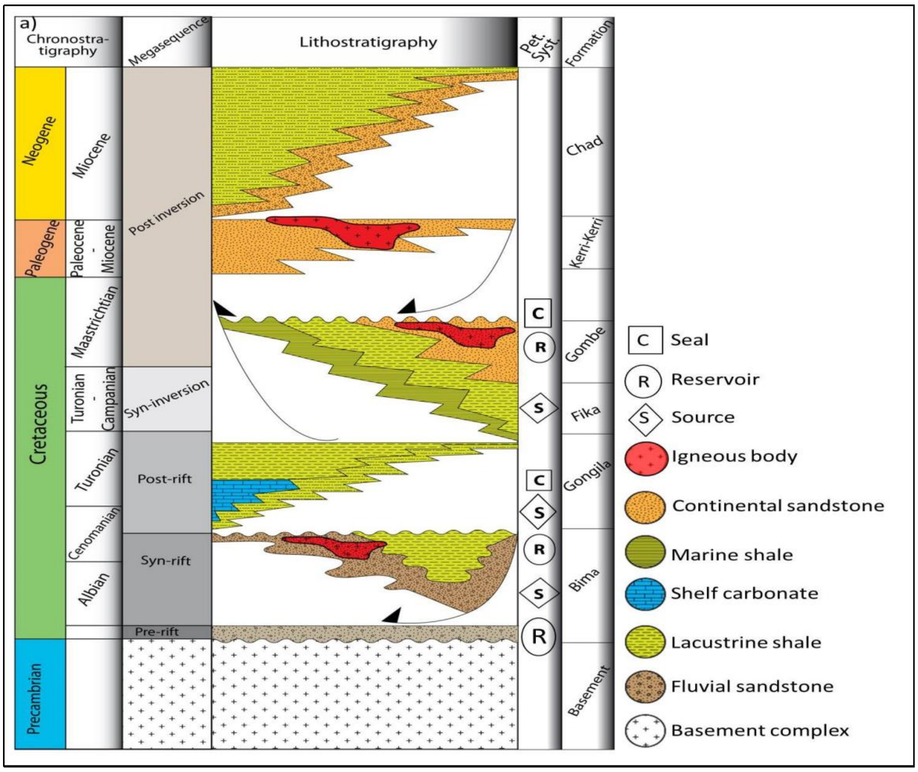

(**a**)

Figure 3. *Cont.*

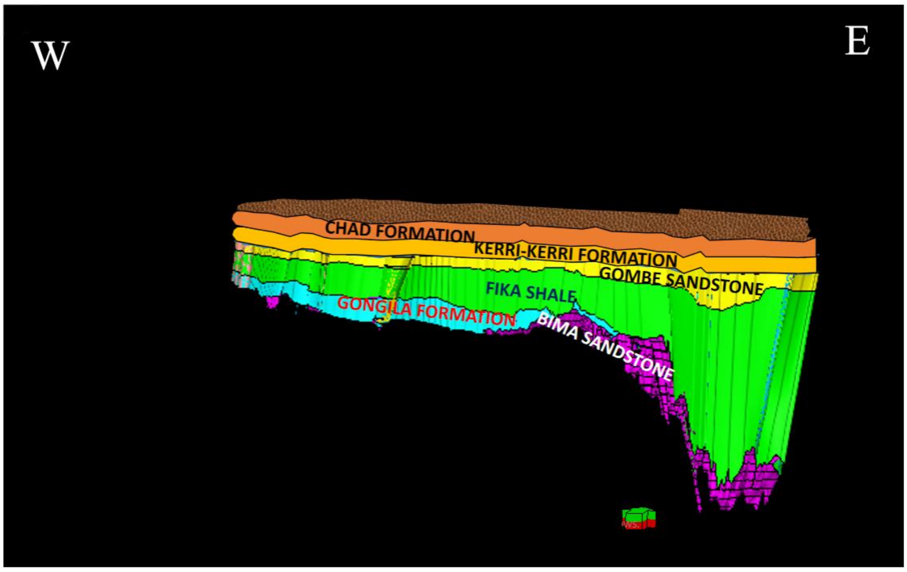

(**b**)

Figure 3. (**a**) Tectonostratigraphy of Bornu Basin showing ages, lithologies, petroleum systems, and (**b**) its geomorphology.

Source: Modified after Suleiman et al. [41].

3. Methodology

The materials (well log data and 3D seismic data) used for this study were obtained from the Nigerian National Petroleum Corporation (NNPC) through the Nigerian Upstream Petroleum Regulatory Commission, formerly the Department of Petroleum Resources (DPR) (see **Table 1**). The fault seal analysis was conducted on a major regional fault structure located proximal to the Bulte-1 well, with the objective of evaluating the sealing integrity of the fault-controlled trap. Fault seal analysis in Move software involves a systematic workflow designed to evaluate the sealing capacity of faults and their impact on hydrocarbon migration and entrapment. The process integrates seismic interpretation, structural modeling, and petrophysical data to quantitatively assess fault-related sealing mechanisms (**Table 2**). The process began with the interpretation of 3D seismic data to identify and map the regional fault system using the Petrel tool (2018 version). Detailed fault mapping was carried out on multiple inlines and crosslines, capturing the spatial continuity, geometry, and orientation of the target fault. Following fault delineation, seismic horizons were interpreted across the faulted seismic sections to map key stratigraphic surfaces. These horizons were correlated with well tops and formation boundaries identified in the Bulte-1 well to ensure accurate stratigraphic control. This correlation established the relationship between primary markers (from well logs) and secondary markers (seismic reflectors), enabling confident time-depth calibration. The following steps outline the standard method used:

Table 1. Data Sources Used in the Study.

Data Type	Source	Purpose in Study
Well log data	Nigerian National Petroleum Corporation (NNPC) via NUPRC (formerly DPR)	Stratigraphic correlation, lithology, petrophysical inputs
3D seismic data	Nigerian National Petroleum Corporation (NNPC) via NUPRC (formerly DPR)	Fault mapping, structural modeling, seismic interpretation

Table 2. Fault Seal Analysis Workflow in Move Software.

Step	Activity	Tools/Inputs	Output/Objective
1	Interpretation of 3D seismic data	Petrel (2018)	Identification and mapping of the regional fault system
2	Fault mapping on inlines and crosslines	3D seismic dataset	Fault geometry, orientation, spatial continuity
3	Seismic horizon interpretation	Seismic sections	Mapping of key stratigraphic surfaces

Table 2. *Cont.*

Step	Activity	Tools/Inputs	Output/Objective
4	Correlation of horizons with well tops and formation boundaries	Bulte-1 well log data	Accurate stratigraphic control
5	Time-depth calibration	Seismic reflectors + well tops	Establish a relationship between primary & secondary markers
6	Structural modeling and petrophysical integration for seal analysis	Move software + well logs	Quantitative fault seal evaluation (SGR, SSF, column height, etc.)

3.1. Fault and Horizon Interpretation

Using 2D or 3D seismic data imported into Move, faults are digitized across multiple sections and interpolated into a 3D fault framework. Stratigraphic horizons are also interpreted and correlated across the faults to generate a complete structural model. This model enables visualization of throw distribution, fault segmentation, and stratigraphic juxtaposition.

3.2. Stratigraphic Modeling and Fault Surface Construction

With the interpreted horizons and faults, a stratigraphic model is built. The software automatically generates fault surfaces and calculates key structural parameters, such as vertical separation, fault throw, and displacement profiles. These are essential inputs for fault seal property calculations.

3.3. Shale Volume (Vsh) Analysis

Vsh values are derived from gamma ray logs and imported into Move as well as log properties. These are assigned to the relevant stratigraphic layers and mapped across the fault surface using interpolation techniques. According to Fisher and Knipe [42], Vsh is critical for determining fault seal parameters like Shale Gouge Ratio (SGR) and Shale Smear Factor (SSF).

3.4. Shale Gouge Ratio (SGR) Calculation

SGR is one of the most widely used fault seal predictors. In Move, SGR is calculated by summing the Vshale of all formations that have moved past a point on the fault surface and dividing by the total vertical throw. A high SGR (typically > 20–25%) suggests increased sealing potential due to clay-rich fault rocks [43,44].

3.5. Shale Smear Factor (SSF) and Probabilistic SSF

SSF is calculated using the thickness of shale beds and the fault throw. It evaluates the potential for continuous shale smear along the fault plane. Probabilistic SSF (PSSF) incorporates uncertainties in bed thickness and displacement, providing a range of possible sealing scenarios [45–47].

3.6. Juxtaposition Diagrams

The move generates juxtaposition diagrams that display the lithological contacts across the fault. These diagrams help identify whether reservoir rocks are juxtaposed against seal or other reservoir units, indicating the potential for cross-fault leakage or sealing due to stratigraphic contact [45,48,49]. According to Zhu and Gong [50], fault sealing capacity was assessed based on three main factors: fault throw, material within the fault zone, and pressure conditions. Fault seals are generally classified into two types: hydraulic and capillary seals [51,52], with capillary seals being the more prevalent. Fault throw determines which lithologies are juxtaposed across the fault. For example, a small throw may place reservoir rock against seal rock (good for sealing), while a large throw may place reservoir against reservoir (bad for sealing). Therefore, throw controls the cross-fault contacts, which are key for understanding juxtaposition sealing potential [50]. The sealing effectiveness of a fault largely depends on the lithological composition on either side of the fault and the capillary pressure characteristics within the fault zone.

3.7. Hydrocarbon Column Height Estimation

Based on the SGR distribution and calibrated thresholds from analog data, Move allows users to estimate the maximum hydrocarbon column height a fault can support before leakage occurs. This aids in prospect risking and volumetric assessments.

4. Results and Interpretations

4.1. Primary Markers

The Bulte-1 well log (**Figure 4**) provides stratigraphic and petrophysical evaluation, dividing the subsurface into four shale intervals (A–D) with interbedded sand facies. Lithostratigraphy comprises Chad, Kerri-Kerri, Gombe, and Fika Formations. Key log tracks include gamma ray (GR), resistivity (ILD), density (RHOB), neutron porosity (NPHI), facies, Vshale, and porosity. Shale tops and bases (A–D) frame sand bodies, highlighted in yellow as potential reservoirs due to lower GR and distinct facies. High GR correlates with shale, low GR with sand, while high resistivity indicates possible hydrocarbon saturation. RHOB–NPHI crossplots estimate porosity. Vshale and porosity logs highlight sands with low shale content and good porosity, especially in lower sections, suggesting favorable reservoir quality[53].

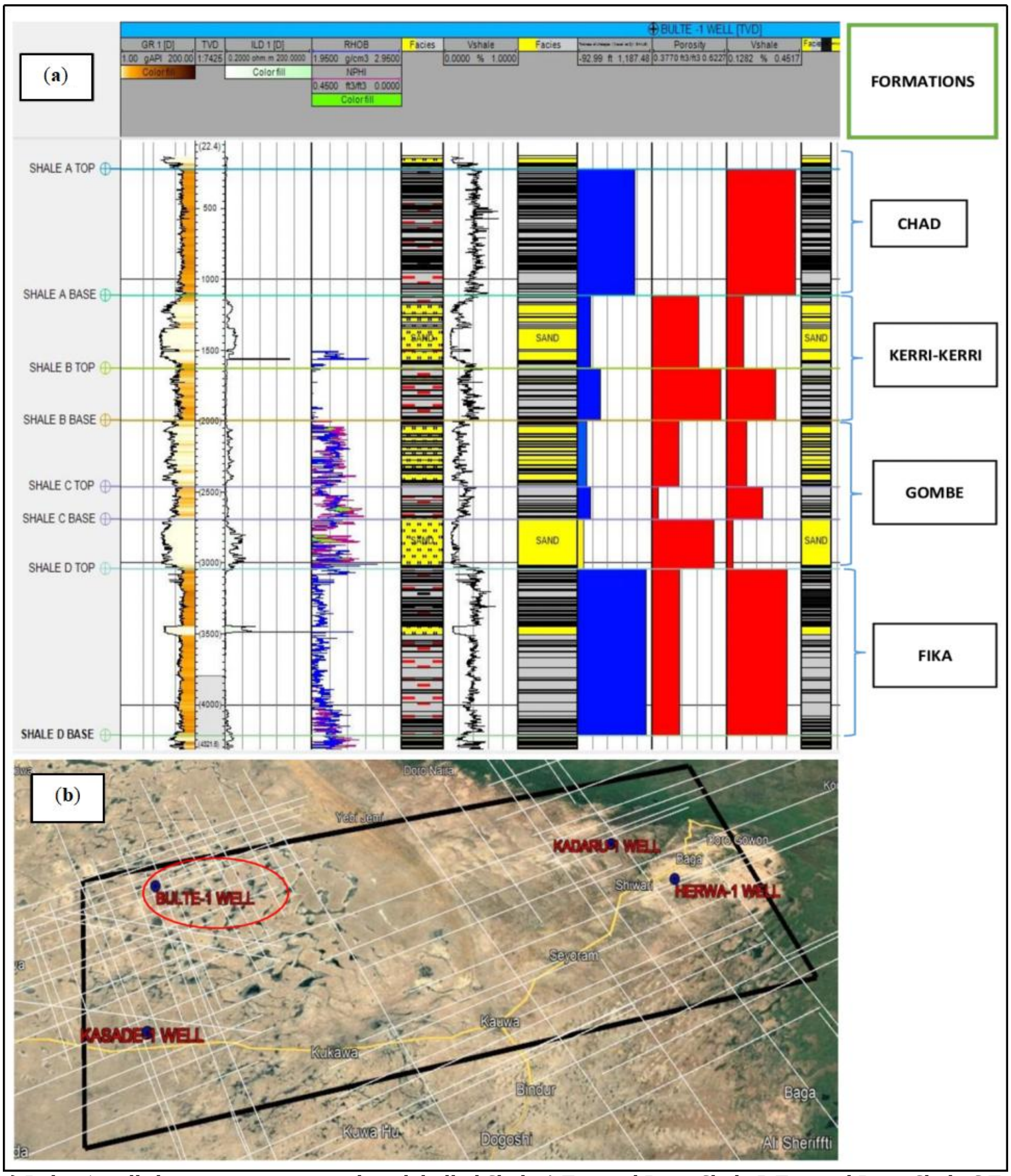

Figure 4. (**a**) Bulte-1 well showing primary markers labelled Shale A Top and Base, Shale B Top and Base, Shale C Top and Base, Shale D Top and Base; (**b**) The lower map shows the geographic setting and spatial relation of Bulte-1 to nearby wells (Herwa-1, Kadaru-1 well, and Kasade-1 well).

4.2. Secondary Markers

The seismic interpretation along inline 5927 (**Figure 5**) delineates seven horizons, including the tops and bases of Shale A and Shale D, with fault analysis integrated around the Bulte-1 well. Ten faults (F1–F10) were identified, showing normal and synthetic configurations. Prominent faults (F4, F5, F6, and F9) display significant vertical displacement, potentially serving as migration pathways or structural traps. The Shale D Top structure map, tied to the seismic via a red line, highlights the spatial distribution of these faults and their relationships to Bulte-1, Kasade-1, Kadaru-1, and Herwa-1.

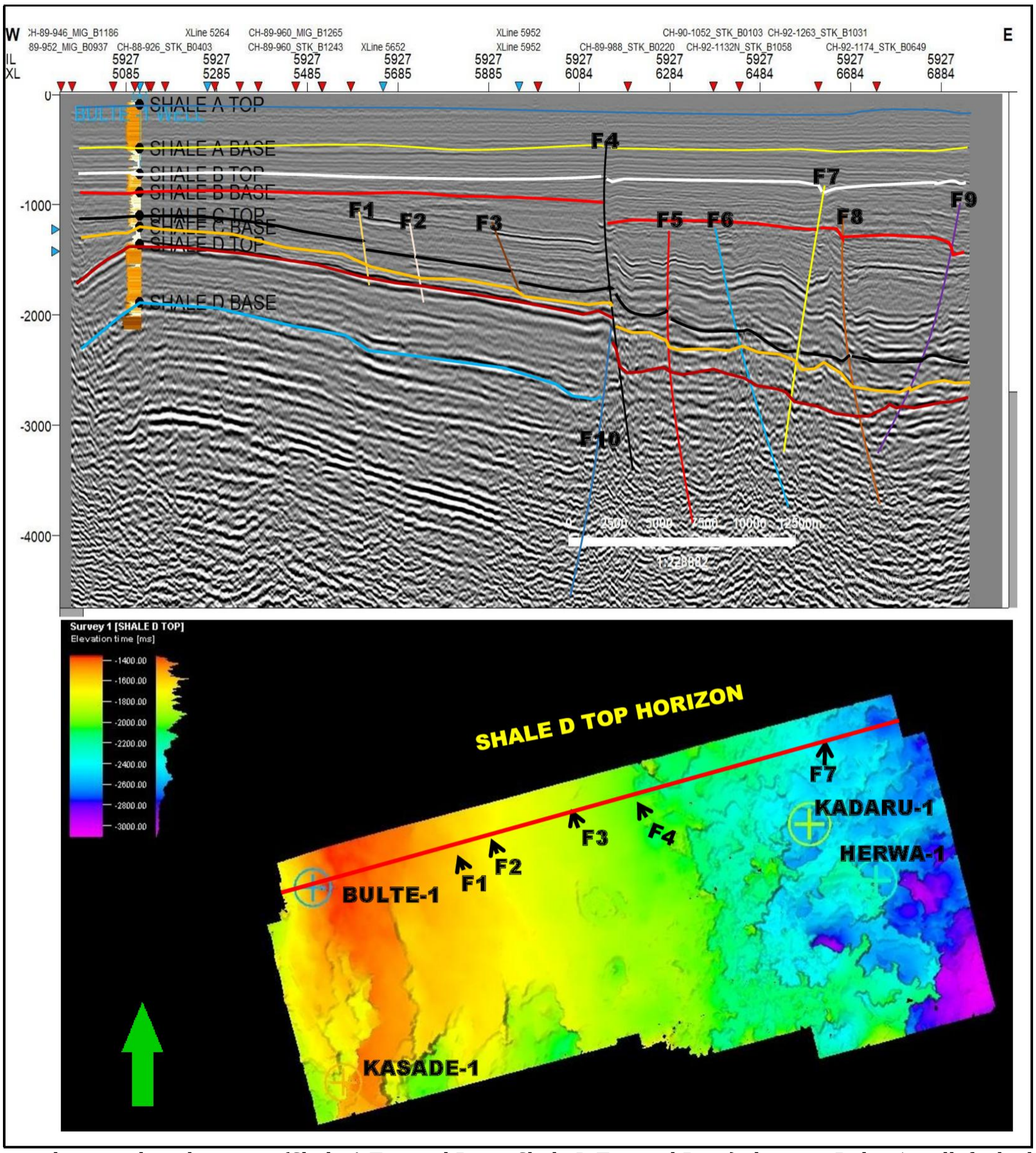

Figure 5. Secondary markers horizons (Shale A Top and Base- Shale D Top and Base) showing Bulte-1 well, faults labelled (F1-F10), and horizon surface generated from Shale D Top with seismic horizon line (Red line).

Note: The red line indicates the position of seismic inline 5927.

Inline 5817 (**Figure 6**) reveals continuation of major faults (F4, F5) and introduces F11–F14 around Bulte-1 and Kasade-1. F12 and F13 show moderate throws near Bulte-1, while the structure map confirms their patterns and regional continuity. Cross-cutting relationships indicate F11 and F14 as the youngest faults; they terminate close to or just below the Shale D Top horizon and lack significant deeper displacement, implying late-stage activity restricted to the shallow section. In contrast, F4, F5, F12, and F13 extend deeper, with F4 and F5 showing large displacements and early tectonic growth. Thus, F11 and F14 are younger, while F4, F5, F12, and F13 represent older tectonic phases.

Inline 5397 (**Figure 7**) emphasizes faults F15–F20, mainly in the western section. Using cross-cutting principles, all faults offset the Shale D Top, making them younger than this horizon. F18 and F20 appear the steepest and most discrete, cutting Shale D Top with minimal vertical growth below, suggesting post-depositional development. F15, F16, and F17 penetrate deeper with gradual growth, indicating earlier faulting initiated during or soon after Shale D deposition. Therefore, F18 and F20 are interpreted as the youngest, while F15–F17 represent older activity.

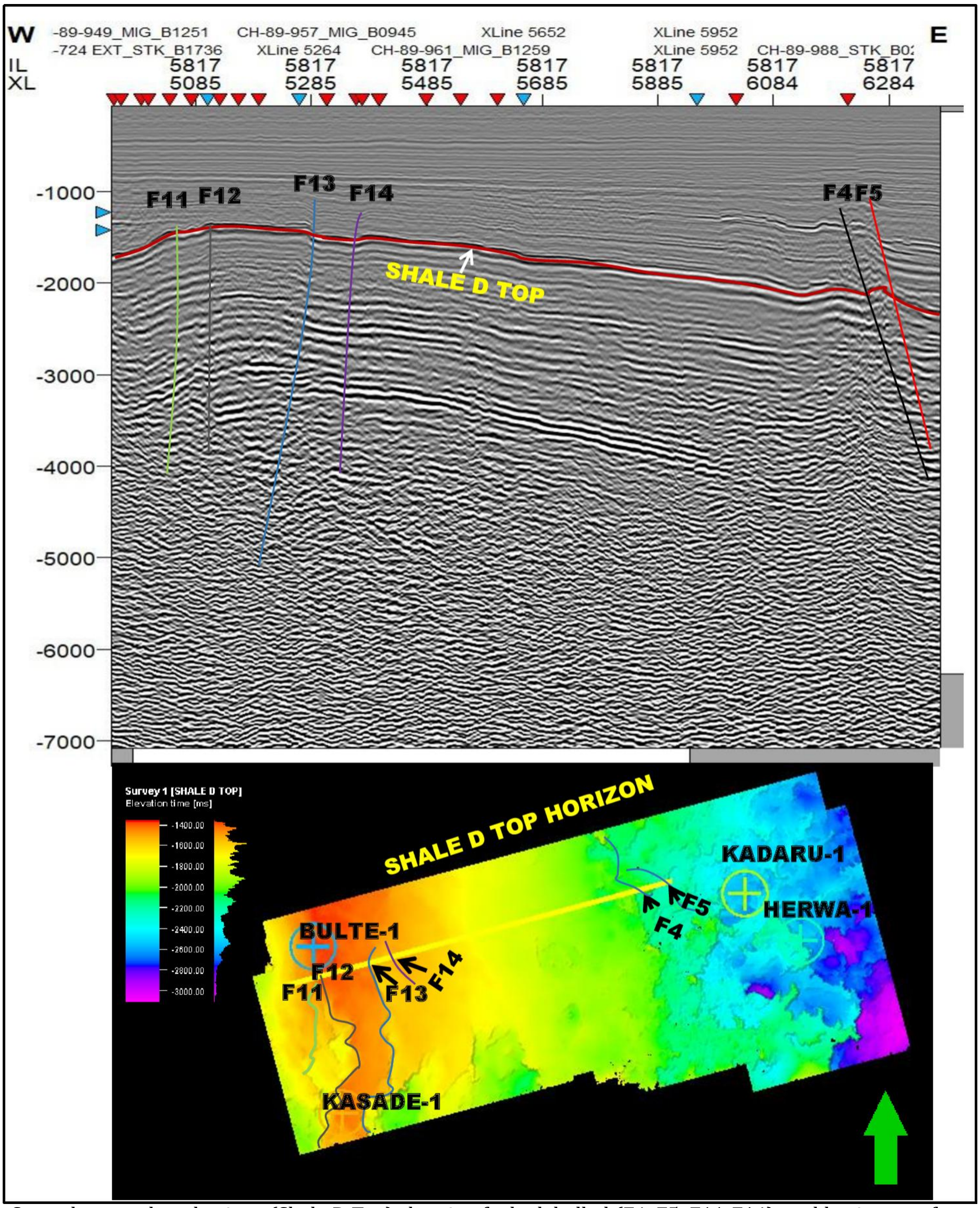

Figure 6. Secondary markers horizon (Shale D Top) showing faults labelled (F4, F5, F11-F14), and horizon surface generated from Shale D Top with seismic horizon line (Yellow line).

Note: The yellow line indicates the position of seismic inline 5817.

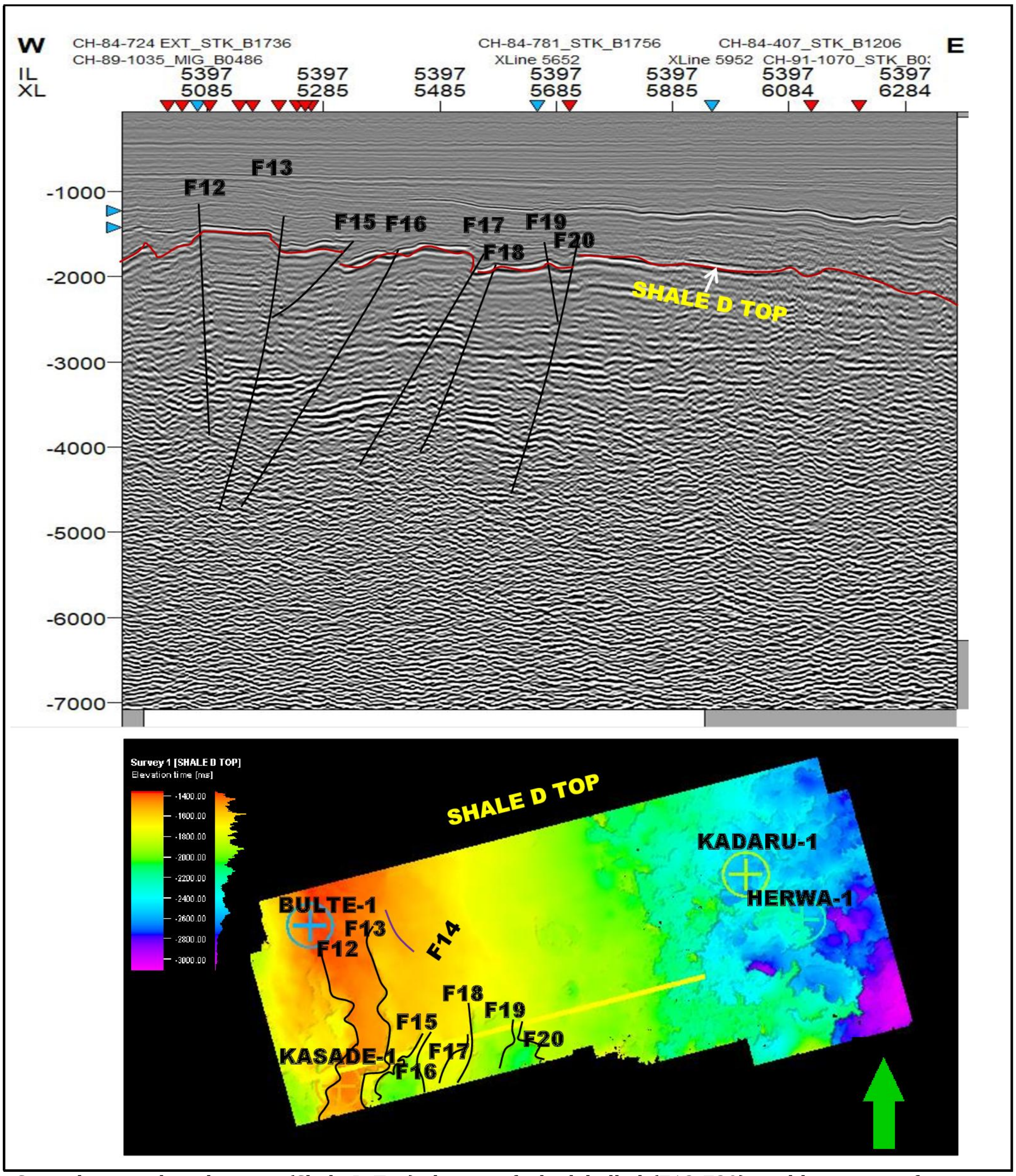

Figure 7. Secondary markers horizon (Shale D Top) showing faults labelled (F12-F20), and horizon surface generated from Shale D Top with seismic horizon line (Yellow line).

Note: The yellow line indicates the position of seismic inline 5397.

In all, the study area is fault-dominated (**Table 3**), with major and minor faults dissecting key horizons. Regionally persistent structures such as F4, F5, and F13 reflect long-term tectonic influence, whereas younger faults indicate post-depositional adjustments. Faults F1–F3 are normal, relatively shallow (950–1165 ft) and short (≈2–2.3 km), indicating extensional deformation. In contrast, F7 and F13 are reverse faults, much longer (7.0–14.9 km) and deeper (≈1014–1221 ft), implying later compressional tectonic activity or inversion of earlier structures. F13, being the longest, likely represents one of the dominant structural boundaries controlling deformation and potential hydrocarbon migration pathways within the study area. The Shale D Top horizon provides a key reference for correlating seismic sections, mapping closures, and evaluating hydrocarbon trap potential within a fault-controlled reservoir framework.

Table 3. Some selected faults from the study area indicating compressional and extensional regions.

Faults	Depth (ft)	Length (m)	Type of Fault	Interpretation
F1	1165.91	2337.3	Normal	Shallow fault of moderate length, indicative of extensional stress regime.
F2	949.96	2080.78	Normal	The shallowest and one of the shorter faults; represents early-stage deformation.
F3	1023.05	2297.56	Normal	Similar depth to F2, consistent with regional extensional tectonics.
F7	1221.30	7060.15	Reverse	Significantly longer and deeper, indicating compressional reactivation or inversion of earlier normal faults.
F13	1013.88	14,895.13	Reverse	The longest fault, suggesting major structural control—likely a principal compressional feature or boundary fault

4.3. Fault Seal Analysis on F13

A total of 48 faults were interpreted and displayed in 3D (**Figure 8**), with different colors representing fault planes and attributes such as throw and dip. Fault F13, a key feature identified in seismic sections, is clearly visualized in the 3D model, confirming its spatial extent and orientation relative to the Bulte-1 well. F13 is emphasized as a major structural element, shown by a yellow line in the seismic section and further analyzed using a rose diagram, which reveals its dominant northeast–southwest strike. The red arrow highlights its primary orientation, offering insights into the regional stress regime and tectonic history. A time-structural contour map of the Shale D Top horizon illustrates elevation variations, with red/yellow contours marking structural highs and blue/purple indicating lows. Bulte-1, Kadaru-1, and Herwa-1 wells are positioned on structural highs, while Kasade-1 lies in a deeper low, consistent with the 3D fault model.

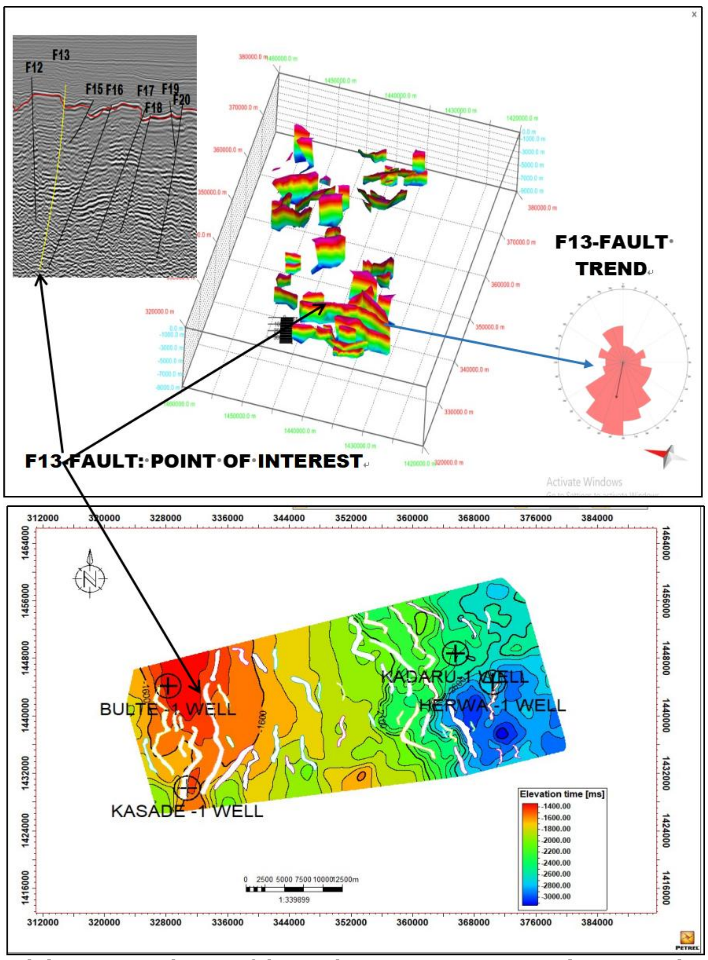

Figure 8. Interpreted faults and the structural time of the study area pointing at northeast trending F13 fault as a very regional fault to be the point of interest for the fault seal analysis.

4.3.1. Lithological Juxtaposition Analysis

The analysis of Fault F13 at the Bulte-1 well (**Figure 9**) provides insights into its sealing capacity. Fault geometry shows displacement increasing with depth, exceeding 4000 ft, confirming its structural significance. Vshale logs from the footwall and hanging wall indicate interbedded sandstones (reservoirs) and shales (seals). Correlating these logs with the juxtaposition diagram highlights depth intervals where sand-shale contacts (red cells) form potential seals, while sand-sand or sand-silt contacts (yellow/orange) suggest leakage zones. The Shale Gouge Ratio (SGR) refines this interpretation: high SGR may provide sealing even in sand-sand juxtapositions by reducing permeability, whereas low SGR in sand-shale contacts can compromise seal integrity. This lithological juxtaposition analysis is crucial for evaluating structural traps, predicting hydrocarbon column height, and assessing lateral seal capacity. It informs well placement by identifying effectively sealed compartments, while highlighting the complex fault seal behavior of F13, shaped by variable sand-shale contacts and SGR values.

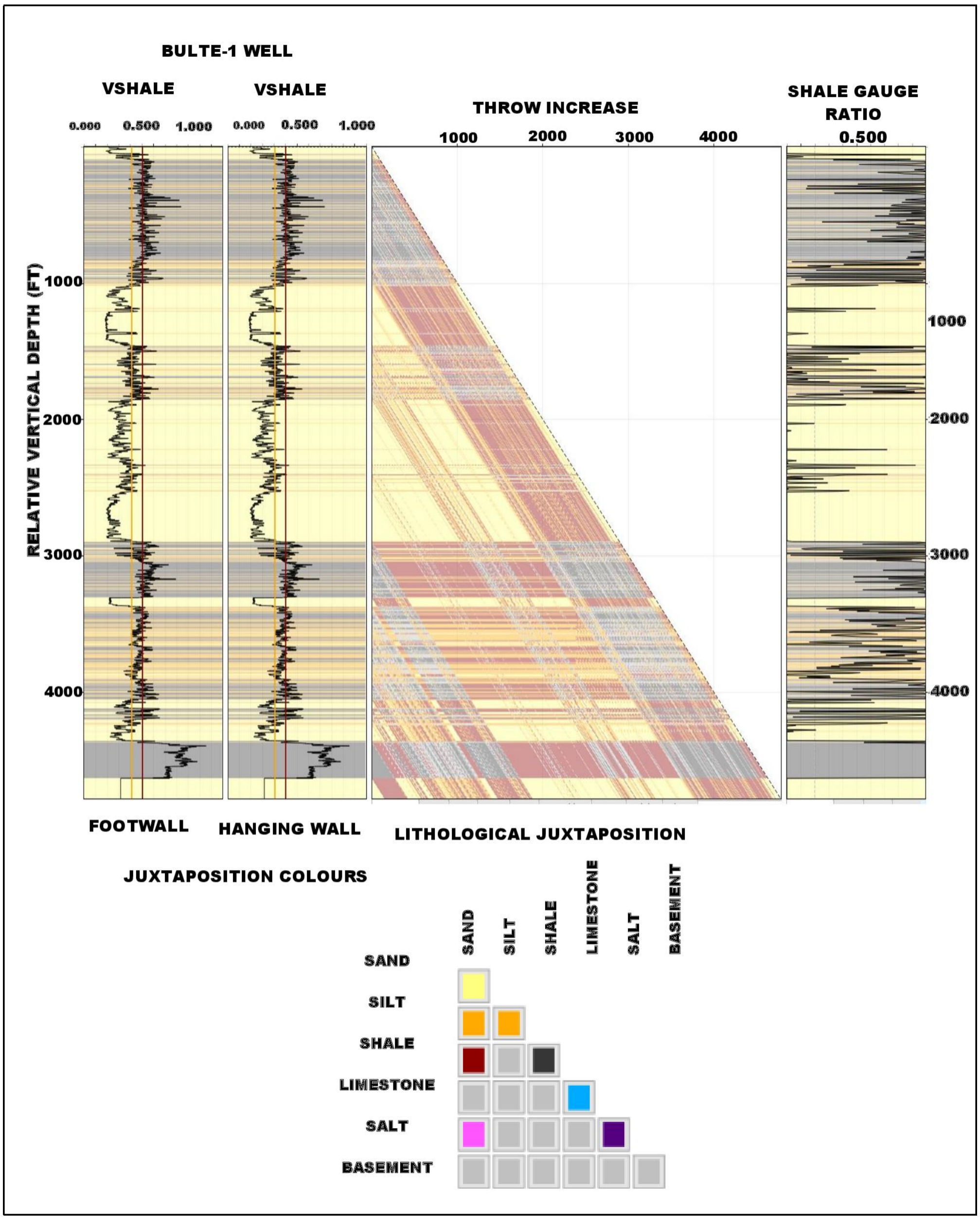

Figure 9. Lithological juxtaposition analysis of the F13-hanging wall and footwall across the Bulte-1 well.

4.3.2. Shale Gouge Ratio (SGR)

The Shale Gouge Ratio (SGR) analysis of the F13 fault at Bulte-1 well provides a quantitative measure of sealing capacity (**Figure 10**). Unlike lithological juxtaposition (**Figure 8**), which shows sand–shale contacts, SGR evaluates how much shale is incorporated into the fault zone. Low SGR values indicate insufficient shale smear and a higher risk of leakage, while high SGR values can create sealing membranes even in sand–sand juxtapositions [44]. Zones with higher SGR (lighter green/yellow/red) suggest effective sealing, capable of supporting larger hydrocarbon columns. Lower SGR areas (darker green) are more permeable, allowing fluid flow and potential hydrocarbon loss. Variations in SGR along the fault plane create compartmentalization, with some blocks sealed and others leaky, resulting in different pressure regimes. This analysis is vital for de-risking exploration, well placement, and pressure management. **Figure 10** demonstrates that sealing effectiveness decreases with depth, directly influencing hydrocarbon trapping and production strategies.

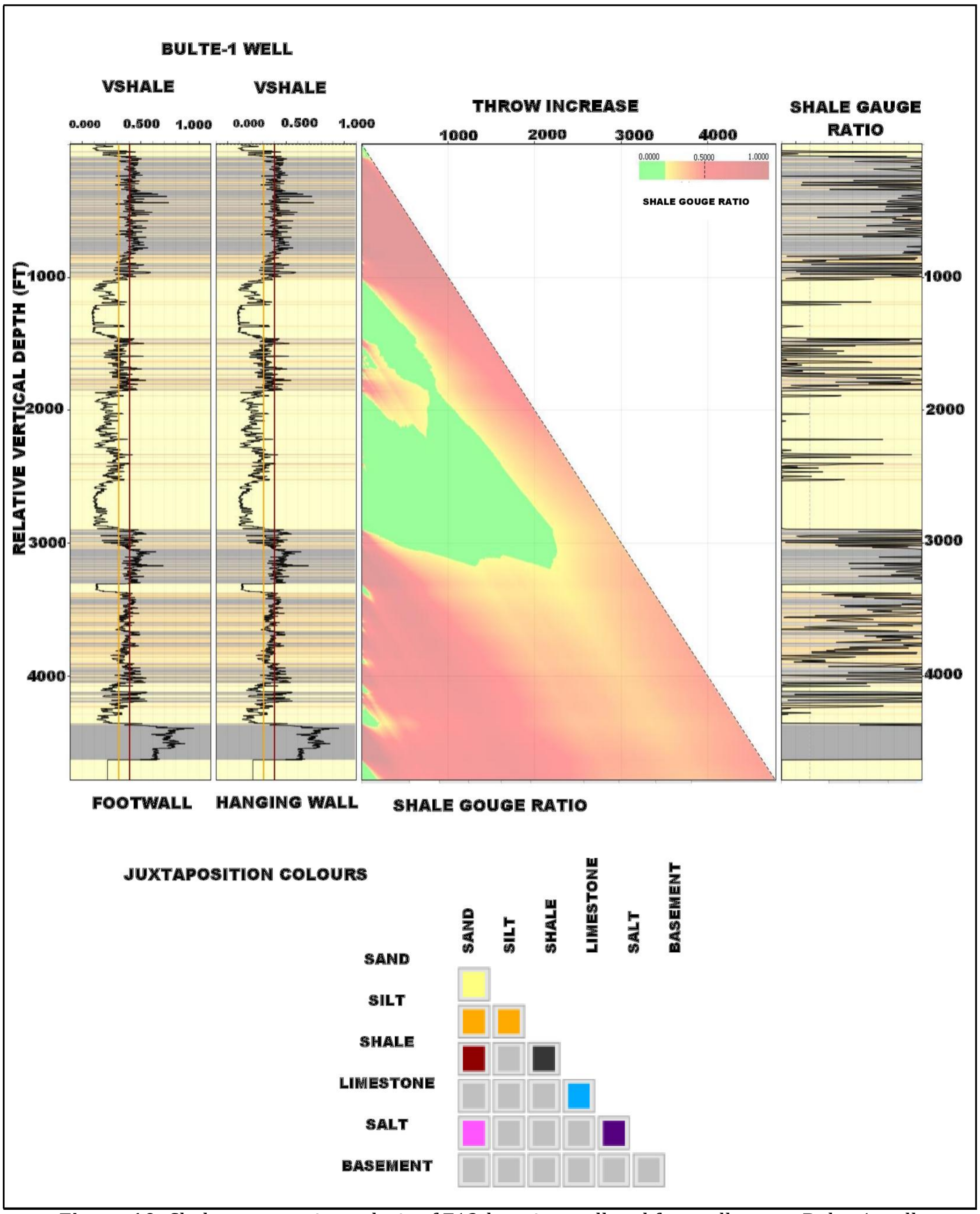

Figure 10. Shale gouge ratio analysis of F13-hanging wall and footwall across Bulte-1 well.

4.3.3. Shale Smear Factor (SMF)

The Shale Smear Factor (SSF) analysis of Fault F13 at the Bulte-1 well reveals essential information about its sealing characteristics (**Figure 11**). SSF works alongside the Shale Gouge Ratio (SGR) and lithological juxtaposition to enhance fault seal evaluation. Low SSF values (dark green) signify continuous shale smears that act as effective seals, commonly found at shallower depths with lower throw or thicker shale intervals. In contrast, high SSF values (light green to red) denote leaky sections, typically occurring at greater depths where high throw disrupts shale continuity. Recognizing these variations is crucial for distinguishing hydrocarbon trapping zones (low SSF) from potential leakage zones (high SSF). Such differences also contribute to reservoir compartmentalization, where a single fault may seal in one interval but leak in another, affecting pressure communication. This analysis aids in minimizing geological uncertainty, optimizing well placement, and improving drainage planning. The sealing efficiency decreases with depth (**Figure 11**), indicating its relevance for exploration and production strategies.

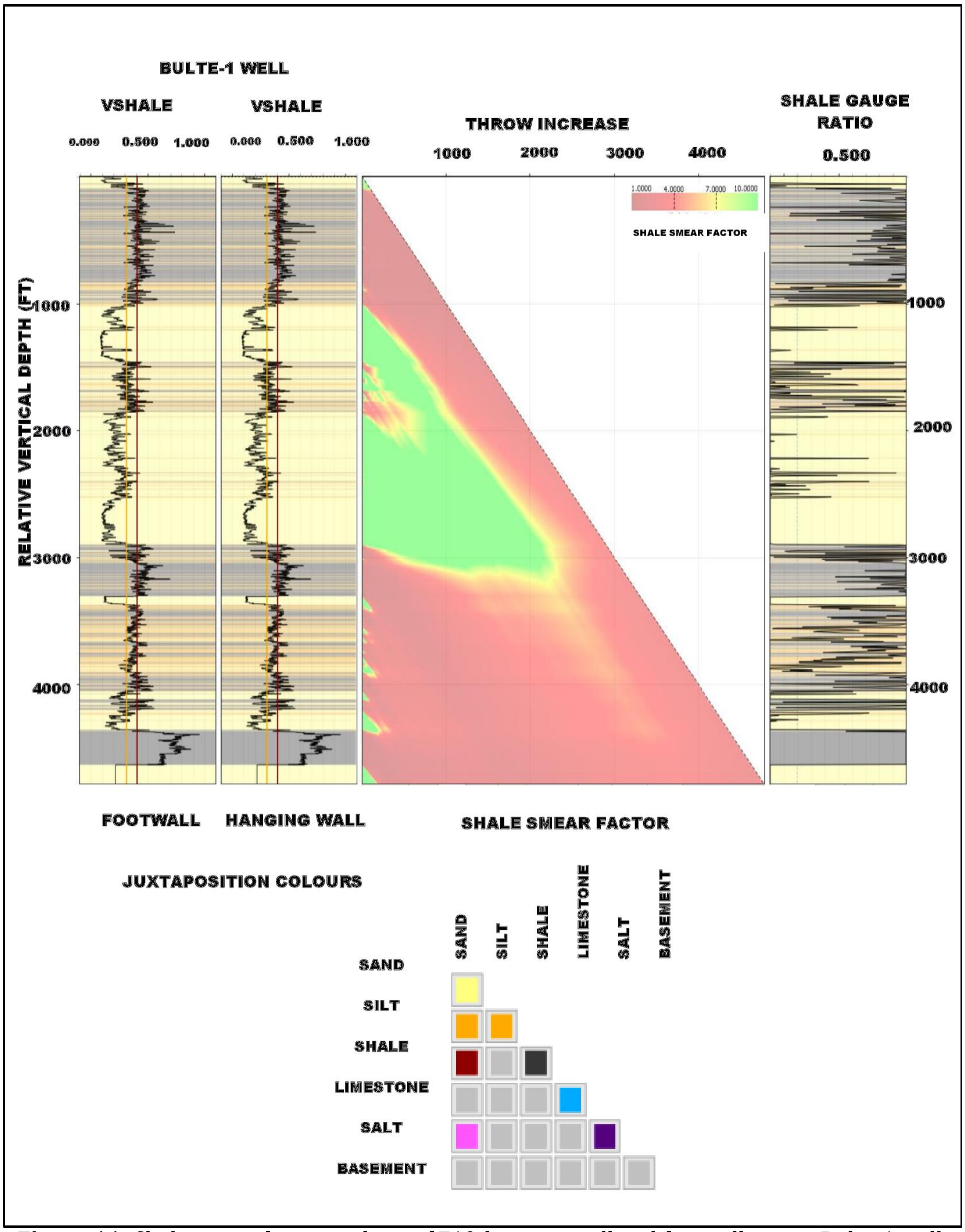

Figure 11. Shale smear factor analysis of F13-hanging wall and footwall across Bulte-1 well.

4.3.4. Probabilistic Shale Smear Factor (PSSF) Analysis

The Probabilistic Shale Smear Factor (PSSF) analysis of Fault F13 in the Bulte-1 well indicates a more realistic evaluation of sealing potential by incorporating uncertainty (**Figure 12**). Unlike the traditional binary seal/no-seal method, PSSF quantifies the probability of sealing, providing direct input for quantitative risk assessment. It assesses shale continuity along the fault plane and complements both the Shale Gouge Ratio (representing bulk shale content) and lithological juxtaposition (depicting rock-on-rock contact). The PSSF diagram differentiates high-probability sealing zones (dark green) from low-probability or leaky sections (light green to red), which is vital for interpreting reservoir compartmentalization. Typically, seal probability decreases with increasing depth and throw, as greater displacements compromise shale continuity. High PSSF regions imply effective sealing and favorable trapping conditions, whereas low PSSF areas indicate possible leakage pathways responsible for dry wells or unanticipated fluid contacts. By quantifying sealing likelihood, PSSF enhances exploration risk evaluation, supports optimal well placement, assists in pressure management, and improves predictions of fault block connectivity for efficient reservoir development.

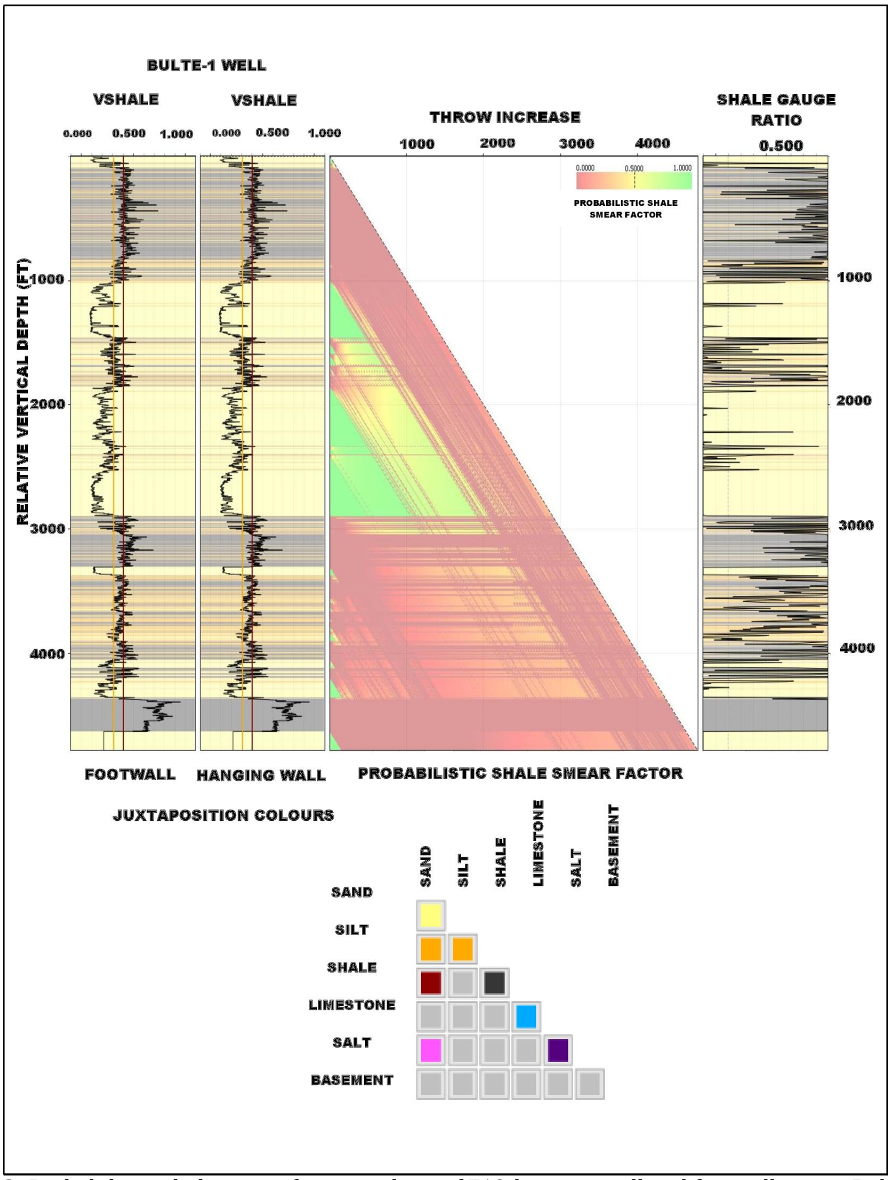

Figure 12. Probabilistic shale smear factor analysis of F13-hanging wall and footwall across Bulte-1 well.

4.3.5. Clay Smear Potential (CSP) Analysis

The Clay Smear Potential (CSP) analysis of Fault F13 in the Bulte-1 well offers a valuable understanding of the fault's sealing efficiency (**Figure 13**). CSP examines how ductile, clay-rich layers are stretched and smeared along the fault surface to form potential sealing barriers. The results identify segments with high clay smear potential (dark green) as effective seals, while low potential areas (light green to red) represent possible leakage zones. Generally, seal potential decreases with increasing depth and throw, as greater displacements disrupt shale continuity. This variation determines the maximum hydrocarbon column a trap can hold before breaching and outlines potential migration pathways. Differences in smear potential lead to reservoir compartmentalization, influencing pressure distribution and fluid contacts, which are critical for production performance. The CSP evaluation assists in assessing exploration risk, optimizing well trajectories, avoiding non-sealing zones, and refining field development plans. At Bulte-1, clay smear effectiveness is highest at shallower levels with relatively small throws.

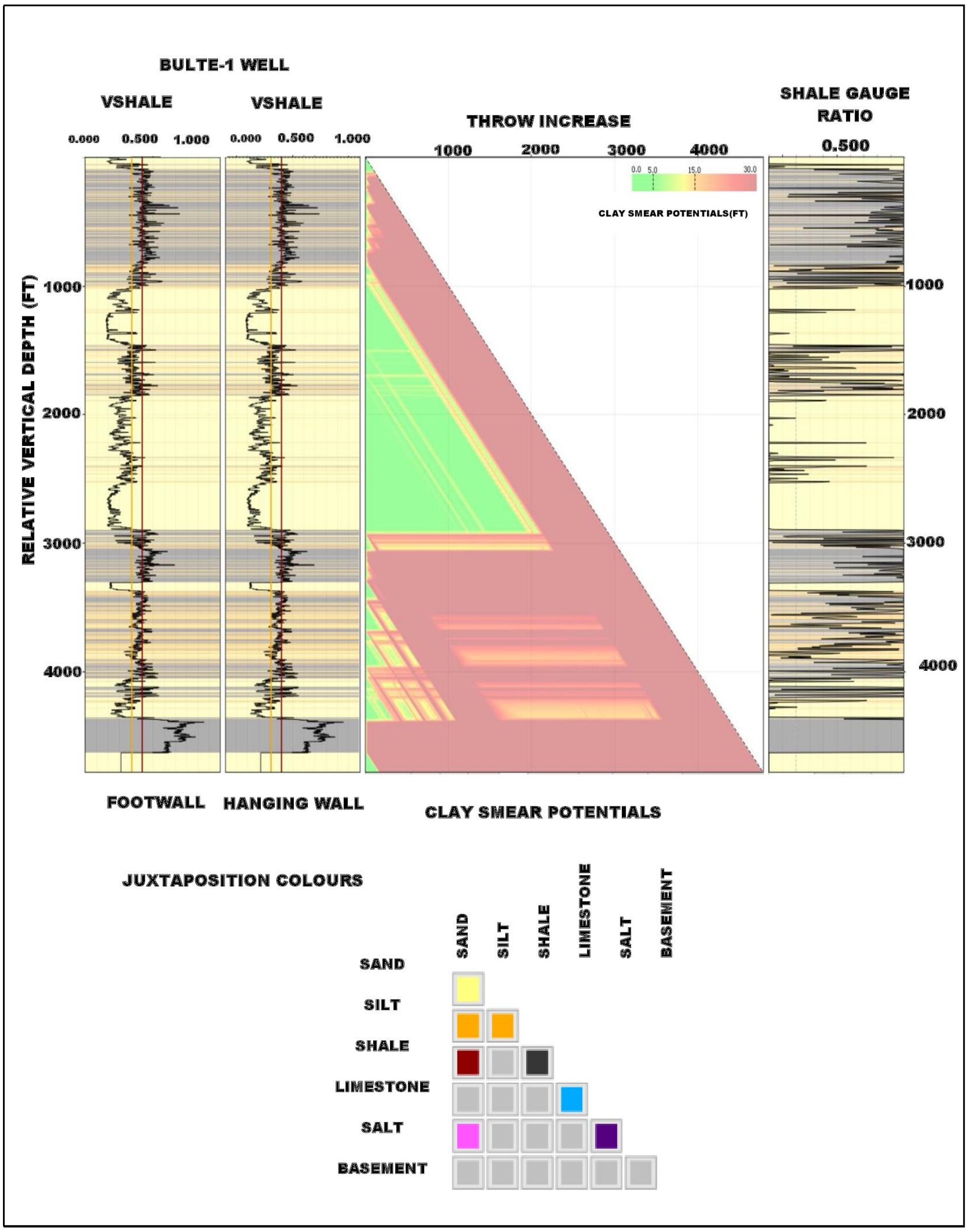

Figure 13. Clay smear potential analysis of F13-hanging wall and footwall across Bulte-1 well.

4.3.6. Permeability Analysis

The permeability evaluation of Fault F13 at the Bulte-1 well represents the concluding phase of fault seal analysis, providing a direct visualization of fluid flow potential across the fault zone (**Figure 14**). Unlike indirect proxies such as the Shale Gouge Ratio (SGR) or Shale Smear Factor (SSF), permeability offers a measurable indicator of seal integrity. Low permeability signifies effective sealing, whereas high permeability indicates potential leakage. Dark blue to purple zones denote strong sealing regions favorable for hydrocarbon entrapment, while red to yellow zones correspond to high-risk leakage pathways. Variations in fault permeability determine the maximum hydrocarbon column height before capillary failure, with low-permeability faults capable of retaining higher columns. Spatial differences in permeability promote reservoir compartmentalization: zones of low permeability isolate compartments and influence pressure and fluid distribution, whereas highly permeable segments facilitate cross-fault communication. This mapping is essential for delineating migration routes, optimizing production and injection well locations, and forecasting reservoir behavior. The results indicate that shallow sections with smaller throws exhibit low permeability and effective sealing, whereas deeper, high-throw areas are more permeable and prone to leakage, impacting trap stability and reservoir management.

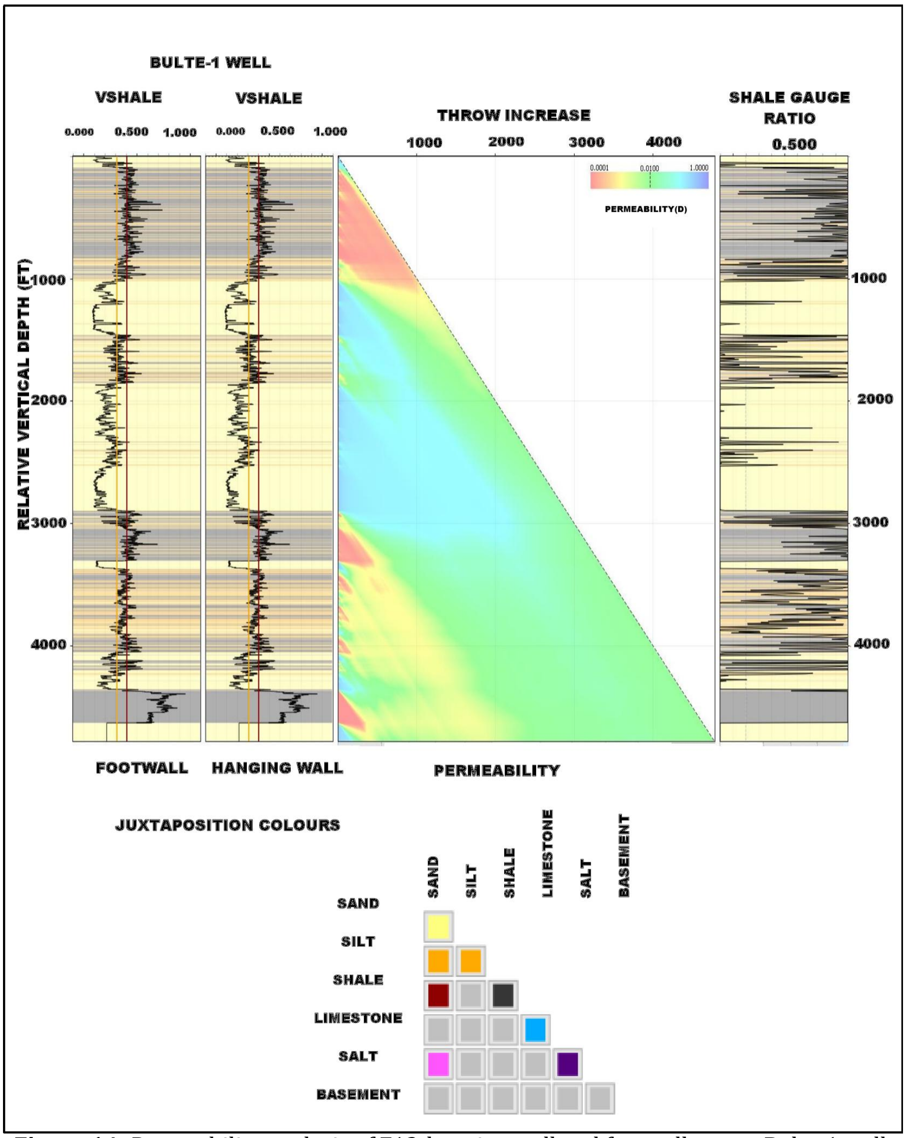

Figure 14. Permeability analysis of F13-hanging wall and footwall across Bulte-1 well.

4.3.7. Hydrocarbon Column Height (HCCH) Analysis

The hydrocarbon column height analysis of Fault F13 at Bulte-1 well is the ultimate predictive output of fault seal studies, directly estimating how much oil or gas the fault can trap (**Figure 15**). The map quantifies trap integrity by predicting maximum hydrocarbon column heights along the fault plane. Dark blue/purple zones represent strong sealing capacity and significant accumulation potential, while red/yellow zones indicate leakage-prone segments. This quantitative approach moves beyond qualitative proxies, providing critical input for volumetric calculations and economic assessments. Variations in predicted column heights highlight reservoir compartmentalization, with different fault blocks sustaining different fill-to-spill points. Low or zero column potential raises prospect risk, while high-column areas guide optimal well placement and pressure management strategies. Results show sealing capacity decreases with depth and throw, reflecting reduced fault integrity. This analysis provides the most direct and actionable measure of fault performance, essential for de-risking prospects and estimating recoverable reserves.

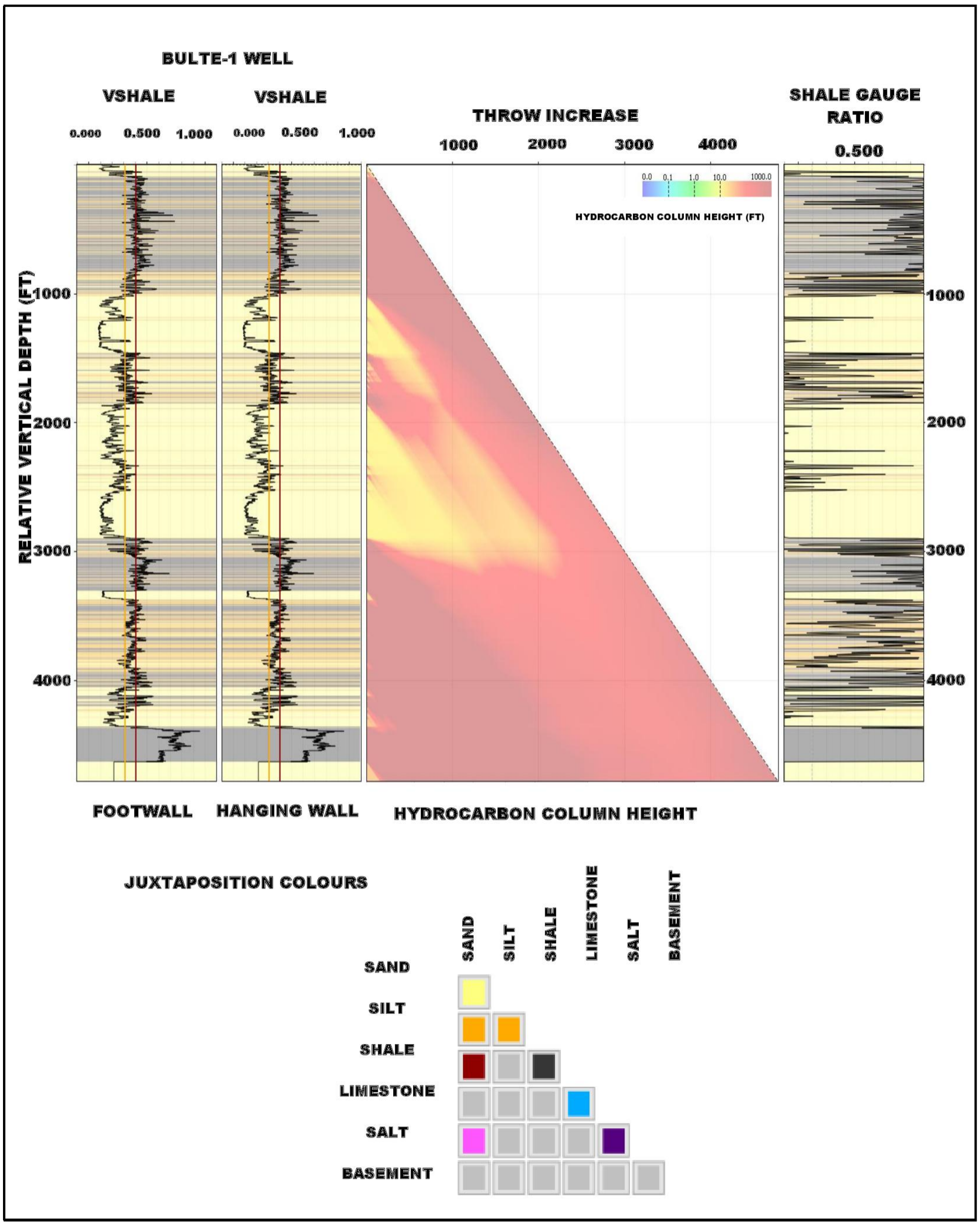

Figure 15. Hydrocarbon column height analysis of F13-hanging wall and footwall across Bulte-1 well.

4.3.8. Volume of Shale Analysis

The Volume of Shale (Vshale) analysis (**Figure 16**) refines the lithological juxtaposition (**Figure 9**) by quantifying shale content across the F13 fault. Instead of broad "sand vs shale" categories, it maps a spectrum of shale proportions, allowing clearer evaluation of sealing potential. Zones where high Vshale (shale) is juxtaposed with shale or with low Vshale (sand/silt) suggest greater sealing potential, particularly when supported by SGR or SSF. Conversely, sand–sand contacts (low Vshale on both sides) highlight likely leakage zones due to high permeability. Vshale data underpins the calculation of SGR and SSF, as more shale increases the likelihood of fault gouge or smear development. This analysis also aids well planning by showing where reservoirs are compartmentalized by sealing shales or directly connected across leaky sand contacts.

The results in **Figure 16** highlight areas where shales are predominantly in contact (suggesting good sealing potential) versus areas where sands are in contact (suggesting leaky potential). This analysis forms a fundamental building block in the comprehensive fault seal assessment, providing the lithological basis upon which more advanced fault seal mechanisms (SGR, SSF, permeability, column height) are calculated and interpreted.

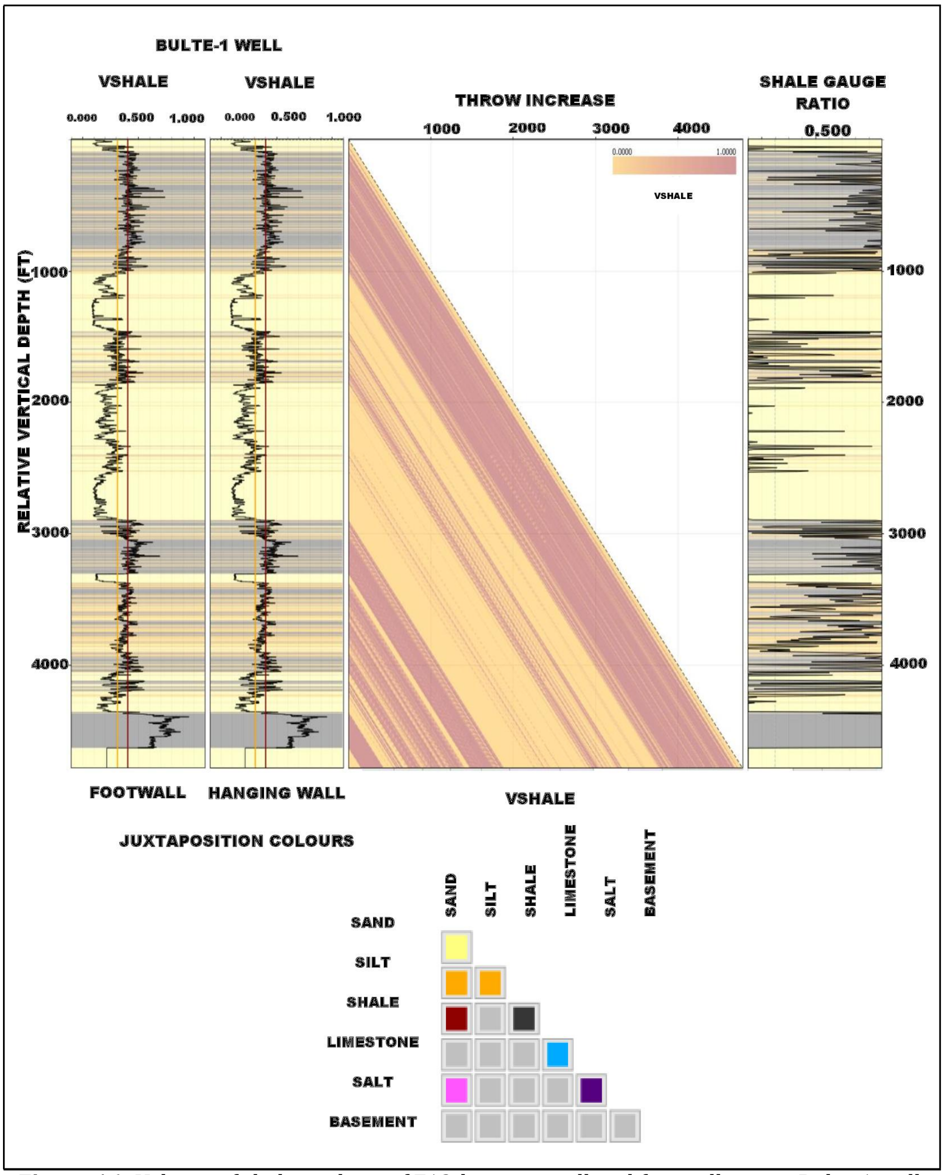

Figure 16. Volume of shale analysis of F13-hanging wall and footwall across Bulte-1 well.

4.3.9. Throw Analysis

The throw analysis (**Figure 17**) provides a fundamental framework for evaluating the F13 fault's sealing behavior at Bulte-1. It illustrates the magnitude and distribution of vertical displacement, which directly controls shale gouge ratio (SGR), shale smear factor (SSF/PSSF), and capillary entry pressure, thereby influencing fault permeability and hydrocarbon column height. Increasing throw with depth identifies F13 as a growth fault, active during sediment deposition, with implications for sediment distribution, basin architecture, and hydrocarbon trapping. Variations in throw also affect lithological juxtaposition, creating complex patterns of sealing and leakage potential. As the throw increases, shale smears become less continuous, reducing sealing efficiency in deeper sections. This analysis also serves as a constraint for seismic interpretation, validating structural complexity and fault growth. In addition, **Figure 17** establishes throw as the critical input for subsequent seal analyses, providing key insights into trap integrity, reservoir compartmentalization, and subsurface hydrocarbon distribution.

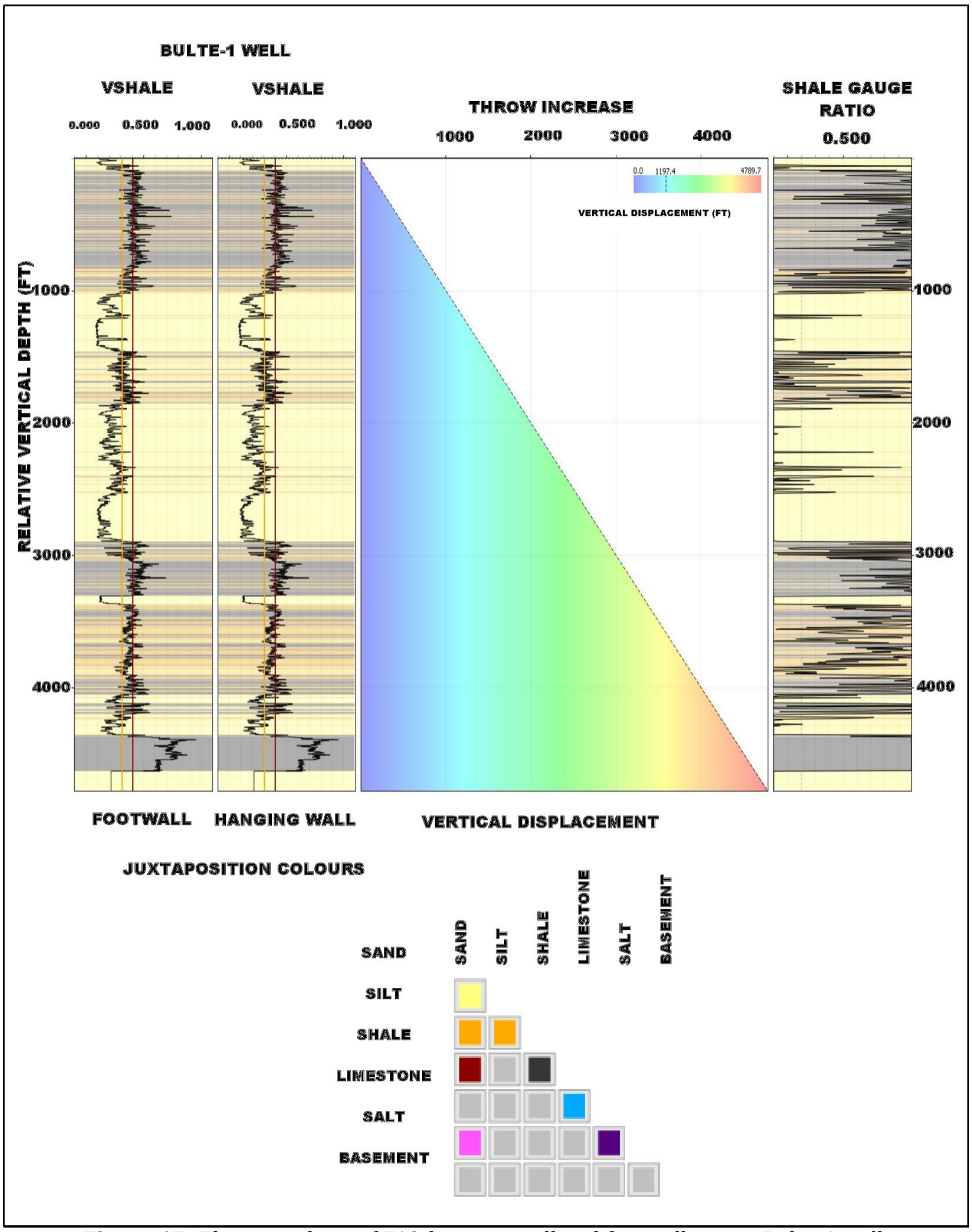

Figure 17. Throw analysis of F13-hanging wall and footwall across Bulte-1 well.

5. Discussion

The Bornu Basin is heavily faulted, and many of these faults are steeply dipping and extensional [12]. Such geometries can result in open fractures that act as conduits for hydrocarbon leakage, thereby compromising trap integrity [7]. The idea that faults may be acting as migration pathways rather than barriers necessitates a detailed evaluation of their sealing potential.

Fault sealing is influenced by various geological parameters including juxtaposed lithologies, fault zone composition, clay content, and throw magnitude [42–44,50]. The study adopts a quantitative approach using advanced geospatial software to model these factors in the F13 fault near the Bulte-1 well, which is identified as a structurally significant feature. Like in the North Sea, fault-related migration and seal integrity are central to successful hydrocarbon discoveries. Similar SGR-based evaluations have been successfully applied in fields like Brent and Forties [42].

The F13 fault exhibits (a) increasing throw with depth, (b) thicker sediment sequences at the downthrown block compared to the upthrown block, (c) strata divergence towards the fault plane, (d) a curved (listric) shape, steep near the surface and flattening with depth, classifying it as a growth fault [54–57]. Lithological juxtaposition analysis shows both sealing (sand-shale) and leaking (sand-sand) contacts, emphasizing compartmentalized behavior. The SGR analysis indicates a range of values along the fault plane, with some zones capable of supporting significant hydrocarbon columns and others prone to leakage. This is because SGR quantifies the amount of shale entrained in the fault gouge. High SGR values (>20–25%) suggest that the fault may form an effective seal [44].

SSF and CSP analyses highlight that deeper sections of the fault, where throw is greatest, are more likely to be leaky. Higher SSF implies a greater risk of fault leakage, especially in deeper sections where throw increases [46]. The probabilistic assessment (PSSF) adds realism by incorporating uncertainties and showing variable sealing probabilities across the fault plane [45–47].

Permeability mapping confirms the heterogeneity in fault sealing behavior, with favorable sealing in shallow regions and potential leak paths at depth. The HCCH analysis supports these conclusions by showing declining column height capacities with depth. These combined results suggest that while the F13 fault has some sealing segments, its deeper portions likely act as migration conduits.

The Termit Basin in Niger and the Doba Basin in Chad have demonstrated successful hydrocarbon accumulations. These basins benefit from greater sedimentary thickness (up to 15 km), more favorable trap-seal relationships, and tectonic stability [40]. In contrast, the Bornu Basin has thinner sediments, signs of intrusive magmatic activity, and evidence of early hydrocarbon generation before trap formation [14]. The Bornu Basin may have experienced less intense rifting and shorter subsidence duration compared to the Termit and Doba basins. This restricted accommodation space for sediment accumulation, resulting in a thinner sedimentary fill (<7 km), is inadequate for deep burial and effective source rock maturation. These geological distinctions may explain the lack of commercial discoveries in Bornu despite similar depositional settings.

Within this context; global and thematic studies on fault seal analysis reveal major advances in understanding how faults influence stress analysis, prospect identification; structural trends; hazard analysis, hydrocarbon migration, accumulation, and trapping and CO_2 storage [58–62]. Reliable fault interpretation and seal assessment are increasingly based on integrating structural, geomechanical, and geochemical models to evaluate fault sealing capacity and hydrocarbon prospectivity [63–67], complemented by machine learning techniques for improved visualization and characterization of fault geometries [68]. Case studies from China, South Africa, Ireland, and Egypt demonstrate the role of stress regimes, shale gouge ratios, and lithological juxtapositions in controlling seal behavior [60,61,63]. Novel approaches such as 3D geomechanical simulations and machine learning models enhance prediction of fault permeability and seal efficiency [69–71]. Many studies also expand applications of fault seal analysis to carbon capture and storage (CCS) and seismic risk evaluation [72,73].

6. Conclusions

The fault seal integrity assessment of the Bornu Basin presents a thorough, methodologically sound evaluation of why commercial hydrocarbons remain elusive in a basin with apparent petroleum potential. By applying advanced structural modeling techniques and integrating seismic, petrophysical, and geological data, the study identifies fault leakage as a plausible explanation for past exploration failures. The results demonstrate that fault seals in the Bornu Basin are heterogeneous, depth-dependent, and influenced by complex tectonic and depositional histories.

The study confirms that fault seal integrity is a significant risk factor in Bornu Basin hydrocarbon exploration. The variability in fault sealing capacity implies that blanket assumptions about trap effectiveness are untenable. Each prospect must be evaluated with site-specific data using a multidisciplinary approach that includes seismic interpretation, well log analysis, and fault modeling.

These insights are valuable for future exploration strategies, such as:

a. Targeting prospective traps with lower fault throw
b. Avoiding sand-on-sand juxtapositions in high-throw zones

Incorporating fault permeability and column height predictions into volumetric risk assessments. These findings align with global best practices in fault seal analysis and underscore the importance of detailed geomechanical evaluations in frontier exploration regions.

Funding

This project was made possible through the financial support and organizational platform provided by the African Union Commission.

Institutional Review Board Statement

Not applicable.

Informed Consent Statement

Not applicable.

Data Availability Statement

Data will be available on special request.

Acknowledgments

The African Union Commission, which established the Pan African University and provided money for this effort, is greatly appreciated by the writer.

Conflicts of Interest

It is declared by the author that no known conflicting financial interest or personal relationship might have influenced any of the work disclosed in this study.

References

[1] Adepelumi, A.A., Falebita, D.E., Olorunfemi, A.O., et al., 2010. Source-Rock Investigation of the Turonian–Maastrichtian Fika Shale From Wireline Logs, Chad Basin, Nigeria. International Journal of Petroleum Science and Technology. 4(1), 19–42.

[2] Olugbemiro, O.R., 1997. Hydrocarbon Potential, Maturation and Palaeoenvironments of the Cretaceous (Cenomanian to Santonian) Series in the Bornu (Chad) Basin, Northeastern Nigeria. Tuebinger Mikropalaeontologische Mitteilungen. 14, 150. (in German)

[3] Olugbemiro, R.O., Ligouis, B., Abaa, S.I., 1997. The Cretaceous Series in the Chad Basin, Northeastern Nigeria: Source Rock Potential and Thermal Maturity. Journal of Petroleum Geology. 20(1), 51–68.

[4] Alalade, B., Tyson, R.V., 2010. Hydrocarbon Potential of the Late Cretaceous Gongila and Fika Formations, Bornu (Chad) Basin, Northeastern Nigeria. Journal of Petroleum Geology. 33(4), 339–353.

[5] Okeke, S., Khitev, Y., Akpunonu, E., et al., 2025. Integrated Environmental Risk Assessment and Climate Resilience Framework for Water-Saturated Reservoirs: A Petrophysical Approach with Cross-Continental Applications. E3S Web of Conferences. 682, 02005. DOI: https://doi.org/10.1051/e3sconf/202568202005

[6] Okosun, E.A., 2000. Preliminary Assessment of the Petroleum Potentials From Southwest Chad Basin, Nigeria. Borno Journal of Geology. 2(2), 40–50.

[7] Okpikoro, F.E., Olorunniwo, M., 2010. Seismic Sequence Architecture and Structural Analysis of Northeastern Nigeria Chad (Bornu) Basin. Continental Journal of Earth Sciences. 5(2), 1–9.

[8] Mohammed, A.Y., Pearson, M.J., Ashcroft, W.A., et al., 1999. Modeling Petroleum Generation in the Southern Muglad Rift Basin, Sudan. Bulletin of the American Association of Petroleum Geologists. 83, 1943–1964.

[9] Adekoya, J.A., Ola, P., Olabode, S., 2014. Possible Bornu Basin Hydrocarbon Habitat: A Review. International Journal of Geosciences. 5(9), 983–996.

[10] Moumouni, A., Obaje, N., Nzegbuna, A.I., et al., 2007. Bulk Geochemical Parameters and Biomarker Characteristics of Organic Matter in Two Wells (Gaibu-1 and Kasade-1) from the Bornu Basin: Implications on the Hydrocarbon Potential. Journal of Petroleum Science and Engineering. 58(3–4), 275–282.

[11] Sunday, O., Adeyinka, A., Ojo, O.S., 2017. Source Rock Evaluation in the Lake Chad Area of the Bornu Basin, Nigeria. Journal of Petroleum and Environmental Biotechnology. 8(1), 1–9.

[12] Didi, C.N., Osinowo, O.O., Akpunonu, O.E., et al., 2025. Multi-Disciplinary Approach to Evaluate Hydrocarbon Potential in the Bornu Basin, Northeastern Nigeria. Journal of African Earth Sciences. 230, 105742. DOI: https://doi.org/10.1016/j.jafrearsci.2025.105742

[13] Uzoma, P.T., Booth, J., Uzoma, K., et al., 2024. Assessing the Impact of Fault Seal on Hydrocarbon Accumulation: The Result of a Blind Well Test, Onshore Niger Delta. In Proceedings of the SPE Nigeria Annual International Conference and Exhibition, Lagos, Nigeria, 5–7 August 2024. DOI: https://doi.org/10.2118/221652-MS

[14] Ahmed, K., Liu, K., Moussa, H., et al., 2022. Assessment of Petroleum System Elements and Migration Pattern of Borno (Chad) Basin, Northeastern Nigeria. Journal of Petroleum Science and Engineering. 208, 109505. DOI: https://doi.org/10.1016/j.petrol.2021.109505

[15] Genik, G.J., 1991. Petroleum Geology of Rift Basins in Niger, Chad, and the Central African Republic. Bulletin of the American Association of Petroleum Geologists. 75, 1405–1434.

[16] Genik, G.J., 1992. Regional Framework, Structural and Petroleum Aspects of Rift Basins in Niger, Chad and the Central African Republic. Tectonophysics. 213, 169–185.

[17] Didi, C.N., Obiadi, I.I., Okeke, S.E., et al., 2020. Structural Architecture of Chad (Bornu) Basin Using 3-D Seismic Data. IOSR Journal of Applied Geology and Geophysics. 8(4), 42–55.

[18] Adepelumi, A., Alao, O., Ako, B., et al., 2012. Modeling of Hydrocarbon Potential and Thermal Maturity of Gongila Shale, Chad Basin, Northeastern Nigeria. Oil Shale. 29(2), 151.

[19] Fairhead, J.D., 1986. Geophysical Controls on Sedimentation within the African Rift Systems. Geological Society of London Special Publications. 25, 19–27.

[20] Binks, R.M., Fairhead, J.D., 1992. A Plate Tectonic Setting for Mesozoic Rifts of West and Central Africa. Tectonophysics. 213, 141–151.

[21] Fairhead, J.D., Green, C.M., 1989. Controls on Rifting in Africa and the Regional Tectonic Model for the Nigeria and Niger Rift Basins. Journal of African Earth Sciences. 8, 231–249.

[22] Burke, K.C., 1969. Seismic Areas of the Guinea Coast Where Atlantic Fracture Zones Reach Africa. Nature. 222, 655–677.

[23] Avbovbo, A.A., Ayoola, E.O., Osahon, G.A., 1986. Depositional and Structural Styles in Chad Basin of Northeastern Nigeria. Bulletin of the American Association of Petroleum Geologists. 70, 1787–1798.

[24] Isyaku, A., Rust, D., Teeuw, R., et al., 2014. Remote Sensing and Geosciences Interpretation of Lineaments for Tectonic and Hydrocarbon Studies in the Bornu Basin. In Proceedings of the Third EAGE Exploration Workshop, Abu Dhabi, United Arab Emirates, 6–9 April 2014. DOI: https://doi.org/10.3997/2214-4609.20140059

[25] Guiraud, R., Maurin, J.-C., 1992. Early Cretaceous Rifts of Western and Central Africa: An Overview. Tectonophysics. 213(1–2), 153–168.

[26] Yusuf, S.N., Yenne, E.Y., Faruk, M.U., 2026. Basement Architecture and Structural Styles of Part of the Nigerian Sector of the Chad Basin (Bornu Basin). Journal of African Earth Sciences. 235, 105979. DOI: https://doi.org/10.1016/j.jafrearsci.2025.105979

[27] Sanusi, Y.A., Likkason, O., 2015. Delineation of Deep-Seated Structural Features Beneath Western Parts of Bornu Basin and Its Adjoining Areas Using Aeromagnetic Data. Nigerian Journal of Physics. 26(1), 34–48.

[28] Zaborski, P., Ugodulunwa, F., Idornigie, A., et al., 1997. Stratigraphy and Structure of the Cretaceous Gongola Basin, Northeastern Nigeria. Bulletin des Centres de Recherches Exploration-Production Elf-Aquitaine. 21, 153–185.

[29] Boboye, O., Akaegbobi, I., 2012. Sedimentological and Palyno-Environmental Appraisal of the Late Quaternary Sediments, Northeastern Bornu Basin. Quaternary International. 262(7), 14–19.

[30] Adeigbe, O.C., Abimbola, A.F., 2013. The Cretaceous–Tertiary Clastic Rocks Weathering Indices: A Case Study of Maastrichtian–Paleocene Rock Succession, Bornu Basin, Northeastern Nigeria. International

Journal of Engineering Sciences and Research Technology. 2(2), 122–130.

[31] Adegoke, A.K., Abdullah, W.H., Hakimi, M.H., et al., 2014. Geochemical Characterisation of Fika Formation in the Chad (Bornu) Basin, Northeastern Nigeria: Implications for Depositional Environment and Tectonic Setting. Applied Geochemistry. 43, 1–12.

[32] Adewumi, T., Salako, A.K., Muztaza, N.M., et al., 2022. Mapping of Subsurface Geological Structures and Depth to the Top of Magnetic Basement in Bornu Basin and Its Environs, Northeastern Nigeria. Arabian Journal of Geosciences. 15(18), 1521. DOI: https://doi.org/10.1007/s12517-022-10818-8

[33] Carter, J.D., Barber, W., Tait, E.A., et al., 1963. The Geology of Parts of Adamawa, Bauchi and Bornu Provinces in Northeastern Nigeria. Bulletin of the Geological Survey of Nigeria. 30, 1–108.

[34] Mohammed, Y., Wulo, I.B., Abdullahi, J., et al., 2019. Geomorphometric and Terrain Analysis of the Nigerian Section of the Chad Basin (Bornu Basin), Northeastern Nigeria. Journal of Geography and Geology. 11(4), 1.

[35] Hamza, H., Hamidu, I., 2012. Hydrocarbon Resource Potential of the Bornu Basin, Northeastern Nigeria. Global Journal of Geological Sciences. 10(1), 71–84.

[36] Ekwok, E., Achadu, M., Ugar, I., et al., 2023. Appraisal of the Magnetic and Geothermal Anomalies of Bornu Basin, Northeastern Nigeria Involving Aeromagnetic Data. Global Journal of Geological Sciences. 21(1), 117–128. DOI: https://doi.org/10.4314/gjgs.v21i1.8

[37] Popoff, M., Benkhelil, J., Simon, B., et al., 1983. Geodynamic Approach to the Benue Trough (Nigeria) Based on Field Data and Remote Sensing. Bulletin des Centres de Recherches Exploration-Production Elf-Aquitaine. 7, 323–337. (in French)

[38] Cratchley, C.R., Jones, P.E., Ajakaiye, D.E., 1984. Geophysical and Geological Evidence for the Benue–Chad Basin Rift System. Journal of African Earth Sciences. 2(2), 141–150.

[39] Benkhelil, J., 1988. Structure and Geodynamic Evolution of the Intracontinental Benue Basin, Nigeria. Bulletin des Centres de Recherches Exploration-Production Elf-Aquitaine. 2(1), 29–128. (in French)

[40] Genik, G.J., 1993. Petroleum Geology of Cretaceous to Tertiary Rift Basins in Niger, Chad and the Central African Republic. Bulletin of the American Association of Petroleum Geologists. 77, 1405–1434.

[41] Suleiman, A.A., Magee, C., Jackson, C.A.L., et al., 2017. Igneous Activity in the Bornu Basin, Onshore Northeastern Nigeria: Implications for Opening of the South Atlantic. Journal of the Geological Society. 174, 667–678. DOI: https://doi.org/10.1144/jgs2016-107

[42] Fisher, Q.J., Knipe, R.J., 2001. The Permeability of Faults Within Siliciclastic Petroleum Reservoirs of the North Sea and Norwegian Continental Shelf. Marine and Petroleum Geology. 18(10), 1063–1081.

[43] Childs, C., Manzocchi, T., Walsh, J.J., et al., 1997. Geometric Controls on Fault Zone Flow Conduits and Barriers. Bulletin of the American Association of Petroleum Geologists. 81(10), 1794–1809.

[44] Yielding, G., Freeman, B., Needham, D.T., 1997. Quantitative Fault Seal Prediction. Bulletin of the American Association of Petroleum Geologists. 81(6), 897–917.

[45] Oluwadare, O.A., Ayefohanne, P.H., 2025. Integration of Artificial Neural Network and Move Fault Analysis Model for Predicting Fault Seals: A Case Study in "Swan" Field, Niger Delta Basin. Arabian Journal of Geosciences. 18, 181. DOI: https://doi.org/10.1007/s12517-025-12312-3

[46] Lindsay, N.G., Murphy, F.C., Walsh, J.J., et al., 1993. Outcrop Studies of Shale Smear on Fault Surfaces. Geological Society of London Special Publications. 70(1), 113–123.

[47] Knipe, R.J., Jones, G., Fisher, Q.J., 2004. Faulting, Fault Sealing and Fluid Flow in Hydrocarbon Reservoirs: An Introduction. Geological Society of London Special Publications. 147, 1–6.

[48] Allan, U.S., 1989. Model for Hydrocarbon Migration and Entrapment Within Faulted Structures. Bulletin of the American Association of Petroleum Geologists. 73(7), 803–811.

[49] Hu, X., Lv, Y., Liu, Y., et al., 2023. Quantitative Study of the Lateral Sealing Ability of Faults Considering the Diagenesis Degree of the Fault Rock: An Example from the Nantun Formation in the Wuerxun-Beier Sag in the Hailar Basin, China. Resources. 12(9), 98. DOI: https://doi.org/10.3390/resources12090098

[50] Zhu, W., Gong, J., 2016. Fault Sealing Evaluation and Hydrocarbon Migration Prediction: A Case Study From Bohai Bay Basin, China. Marine and Petroleum Geology. 77, 275–289.

[51] Watts, N.L., 1987. Theoretical Aspects of Cap-Rock and Fault Seals for Single- and Two-Phase Hydrocarbon Columns. Marine and Petroleum Geology. 4(4), 274–307.

[52] Caillet, G., 1993. Fault Seal Analysis in the Sirte Basin (Libya): A Tool for Risk Evaluation. Petroleum Geoscience. 1, 39–48.

[53] Schlumberger, 1989. Log Interpretation Charts, 4th ed. Schlumberger Wireline and Testing: Houston, TX, USA.

[54] Corredor, F., Shaw, J.H., Bilotti, F., 2005. Structural Styles in the Deep-Water Fold and Thrust Belts of the Niger Delta. Bulletin of the American Association of Petroleum Geologists. 89(6), 753–780.

[55] Evamy, B.D., Haremboure, J., Kamerling, P., et al., 1978. Hydrocarbon Habitat of Tertiary Niger Delta. Bulletin of the American Association of Petroleum Geologists. 62(1), 1–39.

[56] Chukwuemeka, E.V., Ogbamikhumi, A., Salami, S.A., et al., 2025. Structural Evaluation and Hydrocarbon Potentials of Emil Field, Offshore Niger Delta Basin. Results in Earth Sciences. 3, 100142. DOI: https://doi.org/10.1016/j.rines.2025.100142

[57] Weber, K.J., Daukoru, E.M., 1975. Petroleum Geology of the Niger Delta. Proceedings of the 9th World Petroleum Congress. 2, 209–221.

[58] Ding, W., Liu, T., Cao, Z., et al., 2024. Current Research Status and Development Trends of Fault Sealing. Petroleum Geology and Experiment. 46(4), 641–656. DOI: https://doi.org/10.11781/sysydz202404647 (in Chinese)

[59] Didi, C.N., Osinowo, O.O., Akpunonu, O.E., et al., 2025. Reservoir Characterization of Kolmani Field, Northeast Nigeria, Using Well Log Data and 3D Seismic Data for Enhanced Hydrocarbon Prospectivity. Arabian Journal of Geosciences. 18, 161. DOI: https://doi.org/10.1007/s12517-025-12302-5

[60] Ji, J., Wu, K., Pei, Y., et al., 2021. Fault Sealing Evaluation of a Strike-Slip Fault Based on Normal Stress: Eastern Junggar Basin, NW China. Energies. 14(5), 1468.

[61] Amponsah-Dacosta, M., Opuwari, M., Titinchi, S., et al., 2025. Fault Seal Analysis for Geological Carbon Dioxide Storage in the Pletmos Basin, Offshore South Africa. Marine Georesources and Geotechnology. 43(1), 1–15.

[62] Andrews, B.J., Mildon, Z.K., Jackson, C.A.L., et al., 2024. Quantifying Fault Interpretation Uncertainties and Their Impact on Fault Seal and Seismic Hazard Analysis. Journal of Structural Geology. 183, 105158.

[63] Aditama, M.R., Laksono, F.A.T., Fadlin, et al., 2025. Structural Framework and Fault Seal Prediction of the Central Slyne Basin Prospect, Irish Atlantic Margin. Geo-Marine Letters. 45(1), 85–101.

[64] Li, K., Zhang, B., Wu, J., et al., 2025. Comprehensive Evaluation of Fault Sealing for CO_2 Geological Storage. Greenhouse Gases: Science and Technology. e70006. DOI: https://doi.org/10.1002/ghg.70006

[65] El-Qalamoshy, T.R., Abdel-Fattah, M.I., Reda, M., et al., 2023. A Multi-Disciplinary Approach for Trap Identification Including Fault Seal Analysis in the Western Desert of Egypt. Geomechanics and Geophysics for Geo-Energy and Geo-Resources. 9, 157. DOI: https://doi.org/10.1007/s40948-023-00699-w

[66] Michie, E.A.H., Schuller, V., 2024. Fault and Top Seals 2022: A Perspective. Petroleum Geoscience. 30(3), 301–310.

[67] Didi, C.N., Osinowo, O.O., Akpunonu, O.E., 2025. Structural Interpretation and Sequence Stratigraphy of Kolmani Field, Northeast Nigeria, Using 3D Seismic Data and Well Log Data for Enhanced Hydrocarbon Prospectivity. Journal of Sedimentary Environments. 10, 893–923. DOI: https://doi.org/10.1007/s43217-025-00249-2

[68] Bönke, W., Alaei, B., Torabi, A., 2024. Data Augmentation for 3D Seismic Fault Interpretation Using Deep Learning. Marine and Petroleum Geology. 162, 106706. DOI: https://doi.org/10.1016/j.marpetgeo.2024.106706

[69] Xu, M., Guo, Y., Mao, H., et al., 2025. Experimental Investigation on the Shear Behavior of Different Faults in Depleted Gas Storage Reservoirs. Applied Sciences. 15(23), 12489. DOI: https://doi.org/10.3390/app152312489

[70] Jiang, M., Jin, Y., Hu, Z., et al., 2025. Prediction and Evaluation of Fault Lateral Sealing Ability: A New Approach to Integrating Comprehensive Controlling Factors Based on BP Neural Network. Journal of Earth Science. 1–18.

[71] Fisher, Q., Kaminskaite, I., del Pino Sanchez, A., 2023. Shale Barrier Performance in Petroleum Systems: Implications for CO_2 Storage and Nuclear Waste Disposal. Geoenergy. 1(1), geoenergy2023-006. DOI: https://doi.org/10.1144/geoenergy2023-006

[72] Holden, N., Osmond, J.L., Mulrooney, M.J., et al., 2022. Structural Characterization and Across-Fault Seal Assessment of the Aurora CO_2 Storage Site, Northern North Sea. Petroleum Geoscience. 28(4), petgeo2022-036. DOI: https://doi.org/10.1144/petgeo2022-036

[73] Wu, L., Thorsen, R., Ottesen, S., et al., 2021. Significance of Fault Seal in Assessing CO_2 Storage Capacity and Containment Risks—An Example From the Horda Platform, Northern North Sea. Petroleum Geoscience. 27(3), petgeo2020-102. DOI: https://doi.org/10.1144/petgeo2020-102